JNeurosci
THE JOURNAL OF NEUROSCIENCE

Research Articles: Behavioral/Cognitive

Change in brain plasmalogen composition by exposure to prenatal undernutrition leads to behavioral impairment of rats

https://doi.org/10.1523/JNEUROSCI.2721-18.2019

Cite as: J. Neurosci 2019; 10.1523/JNEUROSCI.2721-18.2019

Received: 21 October 2018
Revised: 28 July 2019
Accepted: 31 July 2019

Change in brain plasmalogen composition by exposure to prenatal undernutrition leads to behavioral impairment of rats

Abbreviated title: Ethanolamine plasmalogen and behavior

Kodai Hino[1], Shunya Kaneko[1], Toshiya Harasawa[1], Tomoko Kimura[1], Shiro Takei[2], Masakazu Shinohara[3,4], Fumiyoshi Yamazaki[5], Shin-ya Morita[6], Shumpei Sato[5], Yoshihito Kubo[1], Tadaaki Kono[1], Mitsutoshi Setou[5,7,8], Mina Yoshioka[1], Junya Fujino[1], Hiroyuki Sugihara[9], Hideto Kojima[10], Naoto Yamada[11], Jun Udagawa[1]

[1]Division of Anatomy and Cell Biology, Department of Anatomy, Shiga University of Medical Science, Otsu 520-2192, Japan

[2]Department of Environmental Biology, College of Bioscience and Biotechnology, Chubu University, Kasugai, 487-8501, Japan

[3]Division of Epidemiology, Kobe University Graduate School of Medicine, Kobe, 650-0017, Japan

[4]The Integrated Center for Mass Spectrometry, Kobe University Graduate School of Medicine, Kobe, 650-0017, Japan

[5]International Mass Imaging Center and Department of Cellular and Molecular Anatomy, Hamamatsu University School of Medicine, 1-20-1 Handayama, Higashi-ku, Hamamatsu, Shizuoka 431-3192, Japan

[6]Department of Pharmacy, Shiga University of Medical Science Hospital, Otsu, Shiga 520-2192 Japan

[7]Preeminent Medical Photonics Education & Research Center, (1-20-1 Handayama, Higashi-ku, Hamamatsu, Shizuoka 431-3192,) Japan

[8]Department of Anatomy, The University of Hong Kong, (6/F, William MW Mong Block 21 Sassoon Road, Pokfulam, Hong Kong SAR,) China

[9]Division of Molecular Diagnostic Pathology, Department of Pathology, Shiga University of Medical Science, Otsu, Shiga, Japan

[10]Department of Stem Cell Biology and Regenerative Medicine, Shiga University of Medical Science, Otsu, Shiga, Japan

[11]Department of Psychiatry, Shiga University of Medical Science, Otsu 520-2192, Japan

Correspondence

Jun Udagawa, Division of Anatomy and Cell Biology, Department of Anatomy, Shiga University of Medical Science, Otsu 520-2192, Japan. E-mail: udagawa@belle.shiga-med.ac.jp

Number of pages: 44

Number of figures and tables: 6 and 5, respectively

Number of words for Abstract, Introduction, and Discussion: 222, 426 and 1496

Conflict of Interest: None declared.

Acknowledgments

We thank Mr. Kenji Iwabuchi (Department of Stem Cell Biology and Regenerative Medicine, Shiga University of Medical Science) for assistance in the behavioral test.

48 MALDI-IMS was conducted via the Imaging Platform supported by the Ministry of
49 Education, Culture, Sports, Science and Technology (MEXT), Japan and Preppers Co.
50 Ltd.
51

Abstract

Epidemiological studies suggest that poor nutrition during pregnancy influences offspring predisposition to experience developmental and psychiatric disorders. Animal studies have shown that maternal undernutrition leads to behavioral impairment, which is linked to alterations in monoaminergic systems and inflammation in the brain. In this study, we focused on the ethanolamine plasmalogen of the brain as a possible contributor to behavioral disturbances observed in offspring exposed to maternal undernutrition. Maternal food or protein restriction between gestational day (GD) 5.5 and GD 10.5 resulted in hyperactivity of rat male adult offspring. Genes related to the phospholipid biosynthesis were found to be activated in the prefrontal cortex (PFC), but not in the nucleus accumbens or striatum, in the offspring exposed to prenatal undernutrition. Corresponding to these gene activations, increased ethanolamine plasmalogen (18:0p-22:6) was observed in the PFC using mass spectrometry imaging. A high number of crossings and the long time spent in the center area was observed in the offspring exposed to prenatal undernutrition and was mimicked in adult rats via the intravenous injection of ethanolamine plasmalogen (18:0p-22:6) incorporated into the liposome. Additionally, plasmalogen (18:0p-22:6) increased only in the PFC, and not in the nucleus accumbens or striatum. These results suggest that brain plasmalogen is one of the key molecules to control behavior and its injection using liposome is a potential therapeutic approach for cognitive impairment.

Keywords: Hyperactivity; Maternal undernutrition; Plasmalogen phosphatidylethanolamine; Prefrontal cortex

Significance Statement

Maternal undernutrition correlates to developmental and psychiatric disorders. Here, we found that maternal undernutrition in early pregnancy led to hyperactivity in rat male offspring and induced gene activation of phospholipid-synthesizing enzyme and elevation of ethanolamine plasmalogen (18:0p-22:6) level in the prefrontal cortex (PFC). Intravenous injection of ethanolamine plasmalogen (18:0p-22:6) incorporated into the liposome maintained crossing activity and was circumscribed to the center area for a long time period, in prenatally undernourished offspring with aberrant behavior. Furthermore, the amount of ethanolamine plasmalogen (18:0p-22:6) increased in the PFC of the rat after injection. Our result suggests that brain plasmalogen is one of the key molecules to control behavior and that its injection using liposome is a potential therapeutic approach for cognitive impairment.

Introduction

Epidemiological studies have linked maternal stress during pregnancy, including malnutrition, infection, daily life stress, and traumatic events, to the presence of psychological and developmental disorders in offspring (Hoek et al., 1998; Khashan et al., 2008; Kinney et al., 2008; Marques et al., 2015; Fineberg et al., 2016; Kundakovic and Jaric, 2017). A previous study suggested that brain development is disrupted by prenatal exposure to stress, which alters fetal programming by affecting the epigenome, such as via changes to DNA methylation and histone modification, and induces behavioral disturbances (Kundakovic and Jaric, 2017). A postmortem study of the brain of a patient with schizophrenia suggested decreased *Reelin* and *GAD67* expression due to the hypermethylation of their promoter regions, which was led by the upregulation of DNA methyltransferase 1 (*DNMT1*) genes and may be involved in the etiology of schizophrenia (Kundakovic, 2014). Meanwhile, a Dutch famine study reported the relationship between prenatal undernutrition during the first trimester and the increased incidence of schizophrenia (Brown and Susser, 2008). These reports suggest that maternal stress may alter brain function through disturbances in the neurotransmission of certain systems, such as the GABAergic system. In fact, restraint stress on mice during pregnancy leads to the overexpression of DNMT1 and DNMT3a mRNA, which is accompanied by the downregulation of Reelin and GAD67 protein levels, as well as glutamine receptor protein from the hypermethylation of their promoter regions in the frontal cortex. This cascade of events induced a schizophrenia-like phenotype observable in behavioral tests performed on the male offspring after birth (Matrisciano et al., 2013). Prenatal stress is thus associated with a predisposition toward neurobehavioral disorders. Not only restrained stress, but prenatal caloric restriction has

also been shown to affect the dopamine system and neuronal excitability, resulting in a decrease in anxiety-like behavior, while protein restriction results in deficits in pre-pulse inhibition and locomotor activity (Markham and Koenig, 2011; Amaral et al., 2015). Based on these findings, various neurotransmitter systems, including monoamine, GABAergic, and glutaminergic systems, appear to be viable therapeutic targets for treating behavioral disturbances induced by prenatal stress; however, membrane lipids also seemed to differ between the brains of patients with psychiatric disorders and those without such disorders, and little is known regarding the underlying mechanisms of this process (Ghosh et al., 2017). Therefore, we hypothesized that behavioral disturbance due to early prenatal undernutrition is led by aberrant brain phospholipid metabolism via fetal programming. In this study, we focused on alterations in the composition of brain phospholipids that are induced by prenatal undernutrition, and we have identified a candidate phospholipid to control behavior.

Materials and methods

Animals

All animal procedures were approved by the Institutional Review Board of the Shiga University of Medical Science Animal Care and Use Committee (2011-8-1, 2014-3-7, 2015-12-1, and 2019-4-2). For experiments investigating maternal undernutrition, 9-week-old male (body weight [BW], 250–280 g) and 8-week-old female (BW, 160–190 g) Wistar rats were obtained from CLEA Japan, Inc. (Tokyo, Japan). Six-week-old male rats were obtained for experiments involving phosphatidylethanolamine (PE) injection. All rats were housed under a 12-h light:dark cycle (lights were turned on at 08:00) and were allowed to acclimate for greater than 1 week.

Diet

Female rats were acclimated to a standard diet for pregnant rats (AIN-93G), containing 20% casein for 2 days prior to mating, for which each female was housed with one male overnight. We defined gestational day (GD)0 as the day when a vaginal plug was observed. Pregnant rats were randomly assigned to the *ad libitum* (AL) group, the food-restriction (F) group, or the isocaloric, low-protein-diet (LPD) group, and subjected to undernutrition from GD5.5 to GD10.5 or from the day of blastocyst implantation to the day just before the closure of the neural tube (Fig. 1A) (Erb, 2006). In humans, this period is comparable to the days from E6.5 to approximately E30, which is nearing the first half of the first trimester (Bystron et al., 2008; Schoenwolf et al., 2015). Neural stem cells, and not neurons, exist in the telencephalon because this period is prior to neurogenesis (Götz and Huttner, 2005; Bystron et al., 2008). The F group was fed 50% (50F, four dams) or 40% (40F, six dams) of the daily food intake of

149 the AL group (eight dams). The rationale is that daily rations fell to no more than 800
150 kcal during the Dutch famine that occurred between December 1944 and April 1945,
151 representing 40% of rations (>2000 calories) after June 1945 (Roseboom et al., 2001).
152 The LPD group (five dams) was fed a diet containing 9% casein. After delivery, pups
153 were culled to produce litters of eight offspring (four males and four females) per a dam
154 on postnatal day (P)4. During lactation, the dams were fed CE-2, a standard pellet chow
155 for rearing and breeding. Subsequently, the offspring were weaned on P28, and
156 afterward, they were fed CE-2 *ad libitum*. Male offspring were used in this study
157 because male humans show a higher risk of neuropsychiatric or neurobehavioral
158 disorders (e.g., schizophrenia, attention deficit hyperactivity disorder [ADHD], and
159 autism spectrum disorder [ASD]), than females (Aleman et al., 2003; Werling and
160 Geschwind, 2013; Arnett et al., 2015). Furthermore, sex differences in ADHD and ASD
161 may be, in part, genetically mediated (Werling and Geschwind, 2013; Arnett et al.,
162 2015). The male offspring experienced handling once a week after weaning, and body
163 weight of the offspring were measured at 9 and 12 weeks of age.

164 *Preparation of liposomes*

165 Large unilamellar liposomes composed of egg phosphatidylcholine (PC) and
166 C18:0-22:6 plasmalogen PE (PlsEtn) or C16:0-18:1 diacyl phosphatidylethanolamine
167 (POPE) were prepared by the extrusion method (Morita et al., 2008). Briefly, a thin film
168 was obtained by evaporating the lipid chloroform solution and was subsequently
169 hydrated with saline so that the concentrations of egg PC and PE (18:0p-22:6) (Avanti,
170 AL) were 8 mg/mL and 2 mg/mL, respectively, for PE liposomes (PELs). Similarly,
171 mixed solutions of PE (16:0-18:1) and egg PC were prepared at the same concentration
172 as for the POPE liposomes (POPELs). To produce control liposomes (CLs), PC (10

mg/mL) with no PE was prepared. After five rounds of freezing and thawing, the lipid suspension was extruded through a polycarbonate filter with 100-nm pore size.

Behavioral test

Effects of prenatal undernutrition on behavior

From June to October, the locomotor activity of the male offspring was evaluated by the open-field test at 8 weeks of age for the AL (n = 32 from 8 dams), LPD (n = 18 from 5 dams), 50F (n = 13 from 4 dams), and 40F (n = 17 from 6 dams) groups and at 12 weeks for the AL (n = 18 from 5 dams), LPD (n = 19 from 5 dams), and 50F (n = 14 from 5 dams) groups, to examine the impact of maternal undernutrition on behavior. Behavioral data that included device errors in tracing animals were excluded. The apparatus, measuring 90 cm in diameter and 45 cm in height, was used to monitor the behavior of rats, and the behavior was recorded for 10 min under 9 lux of light. Data were analyzed using the Limelight video tracking system (Actimetrics, IL, USA). The distance traveled and the time spent in the center was measured under the following analysis conditions: the open field was divided into the center and peripheral regions so that 1) the center region was bordered by a concentric circle passing through the midpoint of the radius of the open field (Condition 1 and 2) the area of the center region (A1) was the same as that of the peripheral region (A2) (Condition 2). The former condition was selected to allow crossing behavior to be analyzed.

Effects of plasmalogen (18:0p-22:6) on behavior

To examine the effect of PE (18:0p-22:6), the locomotor activity of male rats was evaluated before and after PE (18:0p-22:6) injection (for 8- and 14-week-old offspring, respectively). Rats were assigned to two different groups based on the results of crossing from the open-field test so that rats with similar locomotor activities were

evenly divided among the groups. A PEL or CL suspension (1 mL/kg BW) was injected into the tail vein at 14 weeks of age, and the second injection of liposome suspension was performed 2 days later. The rats in the PEL (n = 6) and CL (n = 7) groups were subjected to the open-field test or the elevated plus maze test (PEL: n = 6, CL: n = 6) 1 day or 4 days after the second injection, respectively. Behavioral data of one CL rat acquired by using the elevated plus maze test was excluded because it included device errors in tracing animals. In the elevated plus maze test, rats were placed in the central square platform facing the closed arms, and their behavior was recorded for 250 seconds under 8, 10, and 4 lux of light at the central square platform, facing the open arms and closed arms, respectively (Hino et al., 2019). Time spent in the open and closed arms was measured in this test. To verify the specific effect of PlsEtn (18:0p-22:6) on behavior, the alteration of locomotor activity was examined before and after POPEL, CL, or saline injection. Male rats were assigned to three different groups based on the results of the crossing analysis, and behavior was evaluated for POPEL (n = 5), CL (n = 5), and saline injection (n = 4) groups. This experiment was conducted separately from the PEL injection study. The experimental groups allocated in this study are listed in Table 2.

Metabolic profiling of plasma and cerebrospinal fluid (CSF)

Blood samples were collected from male offspring (AL: four dams and seven litters, 40F: four dams and six litters) and CSF (AL: four dams and seven litters, 40F: four dams and five litters) at 9 weeks of age. CSF samples that got mixed with blood were excluded from the analysis. Rats were anesthetized with sodium pentobarbital solution (35 mg/kg, intraperitoneally) during the light phase (16:00–18:00). They were placed in a stereotaxic device (KOPF, CA, USA), and 50 μL of CSF was collected immediately

from the cisterna magna. Then, after decapitation, 5 mL of blood was collected in test tubes containing EDTA-2Na. The plasma was collected after centrifugation of the blood at 2,000 × g for 15 min. Samples were stored at −80°C until use.

Hydrophilic metabolites were extracted using the MeOH-$CHCl_3$ method according to the procedure detailed in previous reports (Tsugawa et al., 2011; Nishiumi et al., 2012). Fifty μL of plasma or CSF was mixed with 250 μL of a solvent mixture (MeOH:H_2O:$CHCl_3$, 2.5:1:1, v/v/v) containing 20 μL of 0.25 mg/mL 2-isopropylmalic acid (Sigma-Aldrich, Tokyo, Japan) as the internal standard. The mixture was then shaken at 37°C for 30 min and centrifuged at 16,000 × g for 5 min at 4°C. Then, 225 μL of supernatant was mixed with 200 μL of distilled water, and the solution was centrifuged at 16,000 × g for 5 min at 4°C. The resultant supernatant (250 μL) containing hydrophilic primary metabolites was collected and lyophilized using a freeze dryer. For oximation, 40 μL of 20 mg/mL methoxyamine hydrochloride (Sigma-Aldrich, Tokyo, Japan) dissolved in pyridine was mixed with a lyophilized sample, and the mixture was then shaken at 30°C for 90 min. For derivation, 20 μL of N-methyl-N-trimethylsilyl-trifluoroacetamide (MSTFA) (GL Science, Tokyo, Japan) was added, and the mixture was shaken at 37°C for 30 min. The mixture was then centrifuged at 16,000 × g for 5 min at 4°C, and the resultant supernatant was subjected to gas chromatography–mass spectrometry (GC–MS) analysis.

GC–MS analysis was performed by using a GCMS-QP2010 Ultra device (Shimadzu Co., Kyoto, Japan) with a fused-silica capillary column (CP-SIL 8 CB low bleed/MS; 30 m × 0.25 mm inner diameter, film thickness: 0.25 μm; Agilent Co., Palo Alto, CA, USA). The front inlet temperature was set at 230°C. The flow rate of helium gas through the column was 39.0 cm/s. The column temperature was held at 80°C for 2 min

and then raised by 15°C/min to 330°C and held for 6 min. The transfer-line and ion-source temperatures were 250°C and 200°C, respectively. Twenty scans per second were recorded over the mass range of 85–500 m/z by using the Advanced Scanning Speed Protocol (ASSP, Shimadzu Co., Kyoto, Japan).

Raw data were exported in netCDF format, and peak detection and alignment were performed by using MetAlign software (Wageningen UR, The Netherlands). The resulting data were exported in CSV format and then analyzed with in-house analytical software (AIoutput), which enabled peak identification and semi-quantification by using an in-house metabolite library (Tsugawa et al., 2011; Nishiumi et al., 2012). For semi-quantification, the peak height of a particular ion for each metabolite was normalized to the peak height of the specified ion of 2-isopropylmalic acid (the internal standard).

Brain sections

According to previous reports, lesions in the medial PFC cause alterations in the locomotor activity of rats (Jinks and McGregor, 1997; Fritts et al., 1998). Moreover, the nucleus accumbens (NAcc) and striatum (CPu) receive input from the PFC and are associated with locomotor activity and impulsivity (Moreno et al., 2013; Spencer et al., 2015; Scofield et al., 2016; Zhu et al., 2016; Dahoun et al., 2017). Hence, sections of PFC, NAcc, and CPu were subjected to gene expression and phospholipid analyses, and immunohistochemistry. Male offspring of 9 weeks of age from the maternal undernutrition experiment and male rats injected with PEL or CL at 14 weeks of age (at 10 hours after the elevated plus maze test) were anesthetized and euthanized with sodium pentobarbital solution (100 mg/kg, ip). Brain samples from the AL (four dams and eight litters), 40F (five dams and eight litters), PEL (n = 4), and CL (n = 4) groups

were immediately dissected out and frozen in dry ice. Cryosections of the brain were cut at a thickness of 10 μm before use for gene expression and phospholipid analyses. Greater than eight sections of the prefrontal cortex (PFC) every 200 μm, greater than six sections of NAcc (Nucleus accumbens) every 80 μm, and greater than seven sections of CPu (Caudate putamen) every 80 μm were placed on Platinum Pro (Matsunami, Osaka, Japan) or polyethylene naphthalate membrane slides (Leica Microsystems, Wetzlar, Germany) for immunohistochemistry or gene expression analysis, respectively. Sections at 0.8 mm and 2 mm from the frontal end of the cerebral cortex, a section at 0.32 mm from the anterior end of the NAcc, and a section at 0.48 mm from the anterior end of the CPu were placed on indium tin oxide (ITO)-coated glass slides (Bruker Daltronics, Bremen, Germany) for phospholipid analysis.

Gene expression

The PFC, NAcc, and CPu of male offspring in the AL and 40F groups were dissected and collected from brain sections by a laser microdissection system (LMD6000, Leica Microsystems, Wetzlar, Germany). Gene expression analysis was performed according to the protocol described in the previous report (Kimura et al., 2018). Isolated total RNA was converted to cDNA via reverse transcription (RT) and amplified using the Ovation PicoSL WTA system V2 (NuGEN Technologies, Inc., San Carlos, CA, USA). The mRNA expression levels were estimated using quantitative real-time PCR (RT-qPCR) analysis using a LightCycler 480 system (Roche Diagnostics GmbH, Mannheim, Germany) with SYBR Premix Ex Taq II polymerase (Takara Bio, Kusatsu, Japan). The RT-qPCR reaction was performed in duplicates, and comparative Cq values of the target genes (Table 1) normalized to B2m, a reference gene, were compared between the AL and 40F groups.

293 *Counting microglial cells and activated microglial cells in PFC*

294 In each rat, ten or more brain sections at approximately 4.8 to 2.6 rostral to the bregma
295 were fixed with 4% paraformaldehyde at room temperature for 30 min, incubated with
296 rabbit anti-Iba1 antibody (dilution, 1:500; Wako Cat# 019-19741, RRID:AB_839504)
297 and mouse anti-CD11b (dilution, 1:300; Bio-Rad / AbD Serotec Cat# MCA275R,
298 RRID:AB_321302), and then incubated with goat anti-rabbit IgG (H&L) conjugated
299 with DyLight 488 (dilution, 1:500; Abcam Cat# ab96895, RRID:AB_10679405) and
300 goat anti-mouse IgG (H&L) conjugated with DyLight 549 (dilution, 1:500; Rockland
301 Cat# 610-142-121, RRID:AB_1057533). Sections were stained with
302 4′,6-diamidino-2-phenylindole (DAPI), and the numbers of all Iba1-expressing
303 microglial cells and CD11b-labeled activated microglial cells were counted in the
304 medial PFC by using a fluorescence microscope (IX83, Olympus, Tokyo, Japan). The
305 density of those cells was then compared between offspring in the AL and 40F groups.

306 *Matrix-assisted laser desorption/ionization-imaging mass spectrometry*
307 *(MALDI-IMS)*

308 MALDI-IMS was performed by using the PFC, NAcc, and CPu samples in both
309 experiments as previously described (Hossen et al., 2015; Sugiyama et al., 2015).
310 Tissues on ITO-coated glass slides were subjected to matrix application by the
311 sublimation/deposition method, with 1 g of 9-AA sublimated at 210°C in order for the
312 deposition thickness to reach 1.0 μm by using the iMLayer device (Shimadzu, Kyoto,
313 Japan). Experiments were performed by using a mass microscope, a prototype of the
314 iMScope equipped with a 355-nm Nd:YAG laser (Shimadzu, Kyoto, Japan). Negative
315 ions from a sample area of 30 μm × 30 μm on the PFC, NAcc, and CPu samples were
316 obtained in a mass range of m/z 400 to 1,000. Adjacent sections of a mouse brain as a

317 reference were laid together with rat brain sections of 40F and AL offspring, and the rats
318 injected with PEL and CL and were used to correct for differences in peak intensity due
319 to differences in sample preparation between slides (Fig. 2). The peaks of 52 PE, 16
320 phosphatidylserine (PS), 14 phosphatidylinositol (PI), 10 lysophosphatidylethanolamine
321 (lysoPE), and 4 lysophosphatidylinositol (lysoPI) were detected (Taguchi and Ishikawa,
322 2010). The peak intensity of each individual phospholipid was corrected using the
323 average intensity of the corresponding phospholipid of the mouse references. The
324 average peak intensities of the PFC, NAcc, and CPu, respectively, were compared
325 between the AL and 40F groups and between the PEL and CL groups.
326 To identify the peak assigned at m/z 774.5 as the peak of PE (18:0p-22:6), we
327 performed MALDI tandem mass spectrometry (MS/MS) using the mass microscope
328 described above (Sugiyama et al., 2015) and identified PE (18:0p-22:6) via
329 collision-induced dissociation (CID) (Zemski Berry et al., 2014).
330 *Blood cells*
331 Blood was collected from 14-week-old male rats for the PEL and CL injection
332 experiment. Whole blood cells were washed with saline, applied to a 12-well
333 flexiPERM® plate (Sarstedt, Tokyo, Japan), and affixed to an ITO-coated glass slide
334 (Matsunami Glass Industries, Osaka, Japan), of which the surface was coated with
335 poly-L-lysine (Hossen et al., 2015) to ensure that the blood cells were confluent. Blood
336 cells were centrifuged to attach the cells to the surface of the glass slide, fixed with
337 0.25% glutaraldehyde for 5 min, and rinsed three times with 150 mM ammonium
338 acetate buffer (pH 7.5). Samples were dried and subjected to MALDI-IMS to examine
339 the phospholipid content in the blood cells Briefly, negative ions from a sample area of
340 10 μm × 10 μm were obtained in a mass range of m/z 400 to 1,000. The ratio of the

peak intensity of PE (18:0p-22:6) to the total peak intensity of all lipids was compared between the PEL and CL groups for the blood cells collected from the rats of these groups.

Statistical analysis

All data are presented as means ± standard deviations. Differences in body weight and locomotor activities in the adult offspring between the 40F, 50F, LPD, or AL groups were identified using one-way analysis of variance (one-way ANOVA) followed by Dunnett's multiple comparison test to examine which treatment leads to the disturbance of the body growth and the behavior in the offspring compared with *ad libitum* food access. Analysis of covariance (ANCOVA) was applied to compare changes in behaviors after liposome injection using the behavioral data at 14 weeks of age as the dependent variable, data at 8 weeks of age as the covariate, and group allocation (CL and PEL groups, or CL, POPEL, and saline groups) as the independent variable. Metabolites in plasma and CSF, gene expression levels, the number of microglia, and phospholipid levels in the brain were compared between the 40F and AL groups by using the unpaired Student's *t*-test. Phospholipid levels in the blood cells were compared among CL, PEL, and saline groups using one-way ANOVA followed by Tukey's HSD test. Differences were considered significant when $p < 0.05$ and Cohen's d was calculated to assess the effect size. ANCOVA was performed using JMP version 14.0 software (SAS Institute Inc., Cary, NC, USA). The other statistical analyses were performed using IBM-SPSS Statistics 22.0 software (IBM-SPSS, Inc., Chicago, IL, USA).

Results

Body weight of male rat offspring

No significant difference was observed between the body weight of male offspring of 40F and that of AL, 50F, or LPD at 9 weeks of age. However, the body weight of the male offspring was significantly lower in the 50F and LPD groups ($p = 0.06$ and 0.10, respectively) compared with that of the male offspring in the AL group using Dunnett's test following one-way ANOVA ($p = 0.002$, $\eta_p^2 = 0.159$ for the main effect) (Table 3). The body weight of 50F and LPD male offspring became similar to that of AL offspring at 12 weeks of age (Table 3).

Maternal undernutrition during early pregnancy leads to hyperactivity in rat offspring

To study the effect of nutritional stress during early embryonic stages on postnatal behavior, the open-field test was performed for adult male offsprings delivered from dams that underwent food restriction from GD 5.5 to GD 10.5. In this study, the behavioral tests performed for offspring at 8 weeks of age revealed that the total distance traveled, the distance traveled in the center area, and the frequency of crossings were significantly increased for males from the 40F group ($p = 0.028$, $p = 0.036$, and $p < 0.001$, respectively), the 50F group ($p < 0.001$, $p = 0.004$, and $p < 0.001$, respectively), and the LPD group ($p = 0.026$, $p = 0.030$, and $p = 0.016$, respectively) compared with the corresponding findings for males in the AL group, in which dams were fed *ad libitum*, using Dunnett's test following one-way ANOVA (total distance traveled: $p < 0.001$, $\eta_p^2 = 0.209$; distance traveled in the center: $p = 0.003$, $\eta_p^2 = 0.167$; frequency of crossing: $p < 0.001$, $\eta_p^2 = 0.439$ for the main effect; Fig. 1B–D). There was no significant difference in time spent in the center area among all groups in

Condition 1 of the open-field test (Fig. 1E), but the time spent in the center area was longer for both the 40F (p = 0.015) and 50F (p = 0.037) groups compared with the AL group in Condition 2, where the radius of the center area represented 70% of the open field (Dunnett's test following one-way ANOVA: p = 0.011, η_p^2 = 0. 135 for the main effect; Fig. 1F). Maternal protein restriction during early pregnancy, in part, contributed to the hyperactivity of the offspring. Increased total distance traveled (LPD: $p < 0.001$, 50F: $p < 0.001$), the distance traveled in the center area (LPD: $p < 0.001$, 50F: p = 0.006), the frequency of crossings (LPD: p = 0.001, 50F: p = 0.011), and the time spent in the center area in Conditions 1 (LPD: p = 0.020, 50F: p = 0.015) and 2 (LPD: p = 0.001, 50F: p = 0.019) were observed even at 12 weeks of age for offspring from the 50F and LPD groups compared with the AL group (one-way ANOVA with Dunnett's test), although this parameter was not examined for the offspring of the 40F group (Fig. 1G–K). However, locomotor activity did not correspond to the body weight at 9 and 12 weeks of age (Fig. 1 and Table 3). The p value and effect size for the main effect in one-way ANOVA of locomotor activities at 12 weeks of age were as follows: total distance traveled: $p < 0.001$, η_p^2 = 0. 333; distance traveled in the center: $p < 0.001$, η_p^2 = 0.298; frequency of crossing: p = 0.001, η_p^2 = 0.237; time spent in the center area: p = 0.011, η_p^2 = 0.173 in Condition 1 and p = 0.001, η_p^2 = 0.246 in Condition 2.

Glyco- and amino-metabolisms are altered in the offspring

In this study, metabolome profiling of the plasma and CSF was performed for offspring at 9 weeks of age (after behavioral tests) of the 40F group, which displayed the most severe behavioral changes among the experimental groups (Fig.3-1). The concentration

410 of glycerol, which is the source of diacylglycerol in phospholipids, was increased in
411 blood plasma (p = 0.014, d =1.57) and CSF (p = 0.001, d = 1.50) in the 40F group
412 compared with the AL group (Fig. 3A). In plasma, 1,5-anhydro-D-glucitol (p = 0.038, d
413 = 1.61) and 2-aminoethanol (p = 0.014, d = 1.21) were also increased in the offspring of
414 the 40F group (Fig. 3A and Fig. 3-1). 2-aminoethanol is converted to O-phosphoethanol
415 amine, and finally transferred to diacylglycerol or 1-O-alkyl-2-acyl-*sn*-glycerol to
416 produce PE (Braverman and Moser, 2012; Vance, 2015).

417 *Microglial cell activation in the PFC is not induced by prenatal undernutrition*

418 The cell densities of Iba1-positive microglial cells and those of both Iba1- and
419 CD11b-positive activated microglial cells in the PFC were not significantly different
420 between the AL and 40F groups (Fig. 3B–D). Additionally, no change in the ratio of
421 activated glial cells to total microglial cells was observed between the AL and 40F
422 groups (Fig. 3E); therefore, microglial cell activation was not enhanced by prenatal
423 undernutrition during the early embryonic period.

424 *Expression of genes related to phospholipid biosynthesis is increased in the PFC*
425 *of rats exposed to prenatal undernutrition*

426 To examine the modulation of the phospholipid biosynthetic pathway in the PFC, NAcc,
427 and CPu in offspring (Fig. 4) exposed to maternal undernutrition, gene expression of the
428 enzymes involved in this pathway was examined. In the brain, dihydroxyacetone
429 phosphate (DHAP) is the main precursor of phospholipids. DHAP is synthesized from
430 glucose and serves as a precursor of diacylglycerol, which constitutes the hydrophobic
431 tail of phospholipids such as PC, PE, and PS (Benjamins et al., 2011). Diacylglycerol
432 may be, in part, formed from glycerol, mediated through glycerol 3-phosphate (Fig. 4)
433 (Jenkins and Hajra, 1976). Further, DHAP serves as a precursor of the

ether-phospholipid, plasmalogen (Braverman and Moser, 2012). In the first step of the synthetic pathway of plasmalogen, as well as that for diacyl phospholipids, hexokinase 1 (*Hk1)* is one of the key enzymes in the regulation of the carbohydrate metabolic rate, which converts glucose to glucose 6-phosphate (McKenna et al., 2011). The expression of *Hk1* was enhanced in 40F offspring (p = 0.016, d = 1.68), although phosphofructokinase (*Pfk1*), the rate-limiting enzyme in glycolysis (McKenna et al., 2011), was not different in the PFC between 40F and control offspring (Fig. 5A, 5B, and 5-1). Regarding the synthesis of the hydrophobic tail of phospholipids, the gene expression of the following enzymes related to diacylglycerol and CDP-diacylglycerol synthesis were elevated in the PFC of the offspring of the 40F group: glyceronephosphate O-acyltransferase (*Gnpat*) (p = 0.001, d = 2.32), glycerol kinase (p = 0.016, d = 1.60), glycerol-3-phosphate transferase (*Gpat*) 1, 3, and 4 (p = 0.027, 0.032, and 0.030, and d = 1.46, 1.50, and 1.57, respectively), and phosphatidate cytidylyltransferase 2 (p = 0.045, d = 1.25). Regarding the synthesis of the hydrophilic head of phospholipids, the gene expression of ethanolamine kinase for PE (p = 0.033, d = 1.37), phosphate cytidylyltransferase 1, choline, alpha (*Pcyt1a*) (p = 0.013, d = 1.68) and phosphate cytidylyltransferase 1, choline, and beta (*Pcyt1b*) (p = 0.010, d = 1.73) for PC; and phosphatidylserine synthase 1 (*Ptdss1*) for PS (p = 0.007, d = 1.86) was elevated in the PFC of the offspring of the 40F group (Fig. 5B). In contrast, plasmalogen is synthesized from ethanolamine or choline and 1-O-alkyl-2-acyl-*sn*-glycerol, which is produced from fatty alcohol and 1-O-alkyl-DHAP (Braverman and Moser, 2012). In this pathway, 1-O-alkyl-DHAP is generated from DHAP by GNPAT and alkylglycerone phosphate synthase (AGPS) (Braverman and Moser, 2012). The genes, *AGPS* (p = 0.013, d = 1.71) and *GNPAT*, of

these enzymes were found to be activated whereas the fatty acyl-CoA reductase 1 (*Far1)* gene expression, which is a potential rate-limiting enzyme (Honsho and Fujiki, 2017), was not altered in the offspring of the 40F group compared with that of the offspring of the AL group (Fig. 5B and 5-1). In contrast to the PFC, *Gpat1* ($p = 0.036$, d = 1.39) and *Pcyt1b* ($p = 0.008$, d = 1.65) expression was lower in the offspring of the 40F group than in the offspring of the AL group in the NAcc and CPu, respectively, although the expression of the other genes, which showed altered expression in the PFC, was not changed in the NAcc and CPu (Fig. 5A, B and 5-1). Furthermore, between the offspring of the AL group and the 40F group, in the PFC, no significant difference was observed in the expression of the calcium-independent phospholipase A2 (*iPla2*) gene, which catalyzes phospholipids (Yeagle, 2016), or that of sphingomyelin synthase 1 (*Sgms1*) and sphingomyelin phosphodiesterase 3 (*Smpd3*), which convert PC into sphingomyelin and ceramide (Vance, 2015), respectively (Fig. 5-1). As described above, our results indicated that the genes of enzymes related to plasmalogen, as well as diacyl phospholipids, were activated in the PFC of offspring exposed to prenatal undernourishment. Alternatively, gene expression was not affected with respect to aquaporin 9 (Aqp9; a channel permeable to glycerol and water) (Badaut and Regli, 2004) or major facilitator superfamily domain containing 2A (Mfsd2a; the major transporter for docosahexaenoic acid [DHA]) (Nguyen et al., 2014). Additionally, the expression of apolipoprotein E, which is involved in lipid transport (Liao et al., 2017), was not altered by prenatal undernutrition (Fig. 5-1).

Phospholipid composition is altered in the cerebrum by maternal undernutrition

The peak intensity of m/z 774.5 PE in the PFC of the offspring of the 40F group was 6.6-fold higher than that of the offspring of the AL group ($p = 0.012$, d = 2.33; Fig. 5C

and D). CID of m/z774.5 yielded product ions at m/z 283.2, 327.2, and 464.3; therefore, m/z 774.5 was identified as PE (18:0p-22:6) (Fig. 5E). Additionally, lysoPE (20:1) in the PFC of 40F offspring was 1.7-fold that of the AL offspring (p = 0.037, d = 1.36); however, no significant difference was observed between groups for the other phospholipids examined (Fig. 5-2). In contrast, the peak intensities of PE (20:1-22:6), lysoPE (20:4), and lysoPE (22:6) in the NAcc (p = 0.045, 0.034, and 0.031, and d = 1.30, 1.39, and 1.42, respectively), and of lysoPE (20:4) and lysoPE (22:6) in the CPu (p = 0.004 and 0.019, and d = 2.07 and 1.57, respectively) were attenuated in the offspring of the 40F group compared with the offspring of the AL group. However, no phospholipid showed enhanced peak intensity in the NAcc and CPu of the offspring of the 40F group (Fig. 5D and 5-2). On the other hand, only PE (18:0p-22:6) in the PFC varied in amount among PlsEtn examined in this study by prenatal undernutrition (Fig. 5D, Table 4). From the perspective of the tail forms of the phospholipids, PE (18:0p-22:6) in the PFC exclusively increased in the offspring of the 40F group among DHA (22:6)-containing phospholipids, although some phospholipids containing DHA or arachidonic acid (AA, 20:4) decreased in the NAcc and CPu (Fig. 5D, Table 4).

PlsEtn affects the behavior of adult rats

To examine the effect of PE (18:0p-22:6) on rat behavior, rats were subjected to the open-field test and elevated plus maze test after intravenous injection of PEL or CL (Fig. 6A). The age-related decline in the frequency of crossing, as well as the difference in the time spent in the center area (Condition 2) was reduced in rats in the PEL group compared with rats in the CL group (Fig. 6B). However, no significant difference was observed in the results of the elevated plus maze test between the PEL and CL groups (Fig. 6D). At the same time, no significant difference was observed in the effect of

POPEL, CL, and saline on rat behavior (Fig. 6C and 6E). Four days after the second injection of PEL (Fig. 6A), the amount of PE (18:0p-22:6) in the PFC ($p = 0.019$, d = 3.02), but not that in the NAcc or CPu, was still greater in the PEL group than in the CL group, while no significant difference was observed in the amount of the other PlsEtn between these groups, as determined by MALDI-IMS (Fig. 6F and Fig. 6-1). The increased amount of PE (18:0p-22:6) in the PFC of the PEL group was verified in another PE injection experiment (Fig. 6-2). Meanwhile, the amounts of PE (22:6-24:6) ($p = 0.019$, d = 3.02), PE (24:4-22:6) ($p = 0.013$, d = 3.36), PS (16:0-22:6) ($p < 0.001$, d = 9.02), PI (16:1-18:1) ($p = 0.004$, d = 4.56), and lysoPE (18:1) ($p < 0.001$, d = 8.58), all of which are acyl phospholipids, were lower in the PFC in the PEL group than in the CL group (Fig. 6F). The amounts of PE (16:0-18:1) (NAcc; $p = 0.041$, d = 2.08, CPu: $p = 0.016$, d = 2.68) and lysoPE (20:1) (NAcc; $p = 0.012$, d = 2.91, CPu: $p = 0.033$, d = 2.64) were lower in the NAcc and CPu for the PEL group than in the CL-group. The amounts of PE (16:1-20:5), PI (18:0-22:4), and plasmalogen PE (18:1p-20:1) were also decreased in the NAcc of the PEL group ($p = 0.008$, 0.032, and 0.023, and d = 3.18, 0.85, and 2.51, respectively), whereas those of lysoPE (18:1), lysoPE (22:6), and lysoPE (22:4) were decreased in the CPu of that group ($p = 0.039$, 0.033, and 0.026, and d = 2.13, 2.55, and 2.42, respectively; Fig. 6F). To verify that increased PE (18:0p-22:6) in the PFC was not ascribed to PE incorporated into the blood cells from liposomes inside blood vessels, PE (18:0p-22:6) in blood cells was measured by MALDI-IMS. The ratio of PE (18:0p-22:6) to total lipids for the PEL group did not differ from that for the CL group (Fig. 6G). Thus, PE (18:0p-22:6) was incorporated at least into the PFC, but not blood cells, after the injection of PE liposomes. Similar to prenatal undernutrition, PE (18:0p-22:6) injection did not increase the amount of other PE, PS,

and PI containing DHA or AA (Fig. 6F, Table 5). Furthermore, most phospholipids that varied in amount after exposure to prenatal undernutrition were not altered by PEL injection, although lyso PE (22:6) was reduced in both 40F offspring and PEL-injected rats (Fig. 5D and 6F, Table 5).

Discussion

The findings of our study suggest that changes in phospholipid composition led by prenatal undernutrition is associated with hyperactivity in rats, and plasmalogen PE (18:0p-22:6) injection reproduces a part of hyperactive behaviors. Regarding the cell membrane, plasmalogens constitute approximately 20% of total phospholipids, both in the rat cerebral cortex and the human brain (Braverman and Moser, 2012). In humans, ethanolamine plasmalogen constitute 57% and 84% of the glycerophosphoethanolamine fraction of the gray and white matter of the frontal cortex, respectively (Braverman and Moser, 2012). Neurons and myelin are rich in plasmalogens, which decrease membrane fluidity, increase membrane rigidity, and allow tight packing of phospholipids in the membrane (Dean and Lodhi, 2017). Plasmalogens play a role in membrane trafficking and fusion processes, Schwann cell differentiation and function, molecule antioxidation, and inhibition of neuronal apoptotic signaling. Hence, a deficiency of plasmalogens induces impairments of neurotransmitter release from synaptosomes to the presynaptic cleft, myelination and axonal sorting by Schwann cells, and neuronal apoptosis signaling (Dean and Lodhi, 2017). These reports suggest the clinical importance of plasmalogens to the nervous system. The amyloid β peptide, which is rich in the brains of patients with Alzheimer's disease, reduces AGPS protein stability and decreases plasmalogen PE levels in patients with Alzheimer's disease (Han et al., 2001; Grimm et al., 2011). Recently, Hossain et al. reported that inflammatory stimuli, such as the administration of lipopolysaccharide (LPS) or polyriboinosinic:polyribocytidylic acid, reduce plasmalogens in murine glial cells through the activation of NF-κB, which downregulates *Gnpat* through increased c-Myc recruitment to the *Gnpat* promoter (Hossain et al., 2017). Similar findings have been observed for the murine brain after

558 aging, exposure to chronic restraint stress, and injection of LPS; furthermore, the
559 reduction of plasmalogen induced activation of microglial cells and elevated expression
560 of proinflammatory cytokines (Hossain et al., 2017). In brains from transgenic mice
561 model of Alzheimer's disease, and postmortem brain tissues from patients with
562 Alzheimer's disease, *Gnpat* reduction via a similar mechanism has been observed
563 (Hossain et al., 2017). Likewise, maternal infection, obesity, a high-fat diet, and
564 restraint stress with bright-light exposure causes microglial cell activation and
565 proinflammatory cytokine induction in the fetal and postnatal brain of rodents and
566 monkeys, and maternal stress results in anxiety-like, depressive and aggressive behavior,
567 and schizophrenia-like behavior in offspring (Bilbo and Tsang, 2010; Grayson et al.,
568 2010; Matrisciano et al., 2012; Diz-Chaves et al., 2013; Sasaki et al., 2013; Marques et
569 al., 2015). In addition, activation of microglia is augmented in the brain including the
570 anterior and orbitofrontal cortices in young adults with ASD, although the distribution
571 pattern of activated microglia is similar to that of healthy control subjects, as
572 determined by positron emission tomography (Suzuki et al., 2013). Maternal obesity
573 before pregnancy is considered a risk factor for ADHD and ASD in humans (Andersen
574 et al., 2017). Obesity is involved in elevated inflammatory mediators, e.g. IL-6, which
575 induces Th17 cell differentiation. IL-17A secreted from Th17 may act to promote ASD
576 by affecting fetal neurodevelopment (Wong and Hoeffer, 2018). These results suggest
577 that brain inflammation plays a key role in behavior and that plasmalogen alters brain
578 function through its anti-inflammatory effects. However, in our study, microglial cell
579 activation was not altered by maternal undernutrition, at least for the adult offspring.
580 Further, injection of plasmalogen PE (18:0p-22:6) to adult rats in the 40F group altered
581 the phospholipid composition and resulted in two characteristic behaviors: frequent

582 crossing and long time spent in the center area in the open-field test.
583 Therefore, the hyperactivity of the rat offspring that were exposed to prenatal
584 undernutrition may be attributable to the phospholipid composition of the brain rather
585 than a direct effect of undernutrition on inflammatory reactions. Patients with RCDP,
586 who display plasmalogen deficiency, have psychomotor retardation, and, in severely
587 affected cases, they display microcephaly and cerebellar atrophy (Berger et al., 2016).
588 Myelination and neuronal migration are thought to be causes of these features of
589 patients with RCDP (Berger et al., 2016). RCDP type 1, type 2, and type 3 are caused by
590 mutations of *PEX7*, *GNPAT*, and *AGPS* (Berger et al., 2016), respectively, all of which
591 contribute to plasmalogen synthesis. In our study, expression of the latter two genes was
592 elevated in the PFC. In RCDP fibroblasts with the *PEX7* mutation, peroxisome targeting
593 signal 2 protein, phytanoyl-CoA hydroxylase, and AGPS fail to be imported into the
594 peroxisome (Yu et al., 2013). The *PEX7* homozygous mutation has also been found in
595 three ASD children whose unaffected siblings were heterozygous or wild-type within
596 one family (Yu et al., 2013). Moreover, single-nucleotide-polymorphism fine mapping
597 has shown that *GNPAT* is a candidate gene for schizophrenia, as is *DISC1* (Liu et al.,
598 2006). These findings suggest that altered phospholipid metabolism, especially
599 plasmalogen metabolism, may be involved in a person's vulnerability to developmental
600 and psychiatric disorders. *Gnpat*-knockout mice show delayed migration of granule cell
601 precursors, enhanced apoptosis in the cerebellum, and hypo- and dysmyelination in the
602 neocortex, cerebellum, and corpus callosum (Berger et al., 2016). Aberrant myelination
603 may be one of the key factors in hyperactivity because MR findings suggest altered
604 myelination in the white matter of adults with ADHD (Wu et al., 2017). Skin fibroblasts
605 derived from patients with RCDP showed reduced PlsEtn, whereas the total amount of

PE was maintained by an increase in other PEs (Dorninger et al., 2015). Polyunsaturated fatty acid (PUFA)-containing PlsEtn was reduced in these cells, and AA-containing, but not DHA-containing, PE species mainly compensated for PlsEtn deficiency (Dorninger et al., 2015). Similar findings have been observed for *Gnpat*-knockout mice; therefore, the ratio among essential PUFAs, as well as the ratio between PlsEtn and PE, may be critical for brain development, and a shift in these ratios may be the cause of the psychomotor retardation of patients with RCDP. In contrast, in our study, the levels of PE (18:0p-22:6) in the PFC and lyso PE (22:6) in CPu were both altered by exposure to prenatal undernutrition and PE (18:0p-22:6) injection. Additionally, injection of POPE, which is not a plasmalogen, did not alter rat behavior. A specific plasmalogen, such as PE (18:0p-22:6), and a specific DHA-containing PE, such as lyso PE (22:6), coupled with the level of plasmalogen in the brain may have a function for behavior. Exogenous administration of plasmalogen can be considered as a potential therapeutic strategy as it results in changes in the phospholipid composition of the brain. Regarding psychiatric disorders, the levels of PUFAs (e.g., PE22:5n6, PC20:3n6, and PC22:5n6) were lower in the white matter adjacent to the dorsolateral PFC of a patient with schizophrenia, while the level of PE20:2n6 was higher, and those of PE22:5n6, PC20:4n6, and PC22:5n6 were lower, in the white matter of the patient with bipolar disorder, despite no alterations in the plasmalogen level for both disorders (Ghosh et al., 2017). A subset combination of the head group (e.g., ethanolamine, choline, serine, or inositol) and a fatty acid tail, such as DHA or AA, which are incorporated into the phospholipid, may be critical to evoke the behavioral alterations that are characteristic of developmental or psychiatric disorders, and thus, could be a therapeutic target to improve conditions for patients with these diseases. As in one of

630 the trials, the administration of a PS supplement in a chewable tablet presentation
631 improved ADHD for children aged 4–14 years (Hirayama et al., 2014). Exogenous PS
632 can cross the blood–brain barrier (BBB) and function in the brain (Glade and Smith,
633 2015). Regarding the delivery of plasmalogen into the brain across the BBB, liposomes
634 with PC may be one of the preferred carriers, since the intravenous injection of
635 liposomes has been the preferred delivery route for many previous studies (Vieira and
636 Gamarra, 2016). However, PE has a cationic head, and the liposome may not be able to
637 reach the brain because of nonspecific binding to the peripheral tissues and serum
638 proteins (Vieira and Gamarra, 2016) if the ethanolamine head is exposed on the surface
639 of the liposome membrane. In our study, the amount of PE (18:0p-22:6) was not altered
640 in blood cells, suggesting that little of the injected PE was taken into the peripheral
641 tissues during circulation in the brain before liposomes were captured by the liver.
642 Plasmalogen is asymmetrically localized to the inner leaflet of the myelin membrane
643 bilayer (Kirschner and Ganser, 1982), and plasmalogen-rich membranes tend to form
644 non-lamellar inverse hexagonal structures compared with the membrane, which
645 exclusively consists of diacyl phospholipids (Dean and Lodhi, 2017). The surface of the
646 liposomes that were used in our study may be electrically neutral, and their nonspecific
647 binding to the peripheral tissues and serum proteins may be prevented.
648 In summary, maternal undernutrition during early pregnancy led to the hyperactivity of
649 male rat offspring, and the behavioral changes observed may be, in part, caused by an
650 alteration of the plasmalogen composition in the PFC, which was induced by the
651 activation of the phospholipid synthetic pathway. Ethanolamine plasmalogen
652 (18:0p-22:6) appears to play a critical role in behavior. Thus, plasmalogens could be
653 candidate therapeutic molecules for improving behavioral disorders. Further study of

654 their complex functions is warranted.

655

656

657 ## Funding

658 This research was supported by JSPS KAKENHI (grant numbers JP 25460242 and
659 16K08441 to JU), the grant from the Food Science Institute Foundation
660 (Ryoushoku-kenkyukai) (to JU), SUMS President's Grant for Encouragement of Young
661 Researchers (grant number 1515503ZU to KH), the SUMS grant for the special research
662 project (grant number 1515503ZZE to JU), the SUMS grant for the integration of basic
663 and clinical research (grant number 1515503ZO to JU), MEXT/JSPS KAKENHI (grant
664 number JP15H05898B1 to MS), and Imaging Platform supported by the Ministry of
665 Education, Culture, Sports, Science and Technology (MEXT) (to MS). FY was
666 supported by Imaging Platform was supported by MEXT.

667

668

669 References

670 Aleman A, Kahn RS, Selten JP (2003) Sex differences in the risk of schizophrenia:
671 evidence from meta-analysis. Arch Gen Psychiatry 60:565-571.
672 Amaral AC, Jakovcevski M, McGaughy JA, Calderwood SK, Mokler DJ, Rushmore RJ,
673 Galler JR, Akbarian SA, Rosene DL (2015) Prenatal protein malnutrition
674 decreases KCNJ3 and 2DG activity in rat prefrontal cortex. Neuroscience
675 286:79-86.
676 Andersen CH, Thomsen PH, Nohr EA, Lemcke S (2017) Maternal body mass index
677 before pregnancy as a risk factor for ADHD and autism in children. Eur Child
678 Adolesc Psychiatry.
679 Arnett AB, Pennington BF, Willcutt EG, DeFries JC, Olson RK (2015) Sex differences
680 in ADHD symptom severity. J Child Psychol Psychiatry 56:632-639.
681 Badaut J, Regli L (2004) Distribution and possible roles of aquaporin 9 in the brain.
682 Neuroscience 129:971-981.
683 Benjamins J, Murphy E, Seyfried T (2011) Lipids. In: Basic Neurochemistry: Principles
684 of Molecular, Cellular, and Medical Neurobiology, 8th Edition (Brady S, Siegel
685 G, Albers RW, Price D, eds), pp81-100: Elsevier Science.
686 Berger J, Dorninger F, Forss-Petter S, Kunze M (2016) Peroxisomes in brain
687 development and function. Biochim Biophys Acta 1863:934-955.
688 Bilbo SD, Tsang V (2010) Enduring consequences of maternal obesity for brain
689 inflammation and behavior of offspring. FASEB J 24:2104-2115.
690 Braverman NE, Moser AB (2012) Functions of plasmalogen lipids in health and disease.
691 Biochim Biophys Acta 1822:1442-1452.
692 Brown AS, Susser ES (2008) Prenatal nutritional deficiency and risk of adult

693 schizophrenia. Schizophr Bull 34:1054-1063.
694 Bystron I, Blakemore C, Rakic P (2008) Development of the human cerebral cortex:
695 Boulder Committee revisited. Nat Rev Neurosci 9:110-122.
696 Dahoun T, Trossbach SV, Brandon NJ, Korth C, Howes OD (2017) The impact of
697 Disrupted-in-Schizophrenia 1 (DISC1) on the dopaminergic system: a
698 systematic review. Transl Psychiatry 7:e1015.
699 Dean JM, Lodhi IJ (2017) Structural and functional roles of ether lipids. Protein Cell.
700 9:196-206.
701 Diz-Chaves Y, Astiz M, Bellini MJ, Garcia-Segura LM (2013) Prenatal stress increases
702 the expression of proinflammatory cytokines and exacerbates the inflammatory
703 response to LPS in the hippocampal formation of adult male mice. Brain Behav
704 Immun 28:196-206.
705 Dorninger F, Brodde A, Braverman NE, Moser AB, Just WW, Forss-Petter S, Brügger B,
706 Berger J (2015) Homeostasis of phospholipids - The level of
707 phosphatidylethanolamine tightly adapts to changes in ethanolamine
708 plasmalogens. Biochim Biophys Acta 1851:117-128.
709 Erb C (2006) Embryology and Teratology. In: The laboratory rat, 2nd Edition (Suckow
710 MAW, Steven H. Franklin, Craig L., ed), pp 817-846. Amsterdam; Boston:
711 Elsevier.
712 Fineberg AM, Ellman LM, Schaefer CA, Maxwell SD, Shen L, H Chaudhury N, Cook
713 AL, Bresnahan MA, Susser ES, Brown AS (2016) Fetal exposure to maternal
714 stress and risk for schizophrenia spectrum disorders among offspring:
715 Differential influences of fetal sex. Psychiatry Res 236:91-97.
716 Fritts ME, Asbury ET, Horton JE, Isaac WL (1998) Medial prefrontal lesion deficits

involving or sparing the prelimbic area in the rat. Physiol Behav 64:373-380.

Ghosh S, Dyer RA, Beasley CL (2017) Evidence for altered cell membrane lipid composition in postmortem prefrontal white matter in bipolar disorder and schizophrenia. J Psychiatr Res 95:135-142.

Glade MJ, Smith K (2015) Phosphatidylserine and the human brain. Nutrition 31:781-786.

Grayson BE, Levasseur PR, Williams SM, Smith MS, Marks DL, Grove KL (2010) Changes in melanocortin expression and inflammatory pathways in fetal offspring of nonhuman primates fed a high-fat diet. Endocrinology 151:1622-1632.

Grimm MO, Kuchenbecker J, Rothhaar TL, Grösgen S, Hundsdörfer B, Burg VK, Friess P, Müller U, Grimm HS, Riemenschneider M, Hartmann T (2011) Plasmalogen synthesis is regulated via alkyl-dihydroxyacetonephosphate-synthase by amyloid precursor protein processing and is affected in Alzheimer's disease. J Neurochem 116:916-925.

Götz M, Huttner WB (2005) The cell biology of neurogenesis. Nat Rev Mol Cell Biol 6:777-788.

Han X, Holtzman DM, McKeel DW (2001) Plasmalogen deficiency in early Alzheimer's disease subjects and in animal models: molecular characterization using electrospray ionization mass spectrometry. J Neurochem 77:1168-1180.

Hino K, Kimura T, Udagawa J (2019) Handling has an anxiolytic effect that is not affected by the inhibition of the protein kinase C pathway in adult prenatal undernourished male rat offspring. Congenit Anom (Kyoto).

Hirayama S, Terasawa K, Rabeler R, Hirayama T, Inoue T, Tatsumi Y, Purpura M, Jäger

741 R (2014) The effect of phosphatidylserine administration on memory and
742 symptoms of attention-deficit hyperactivity disorder: a randomised, double-blind,
743 placebo-controlled clinical trial. J Hum Nutr Diet 27:284-291.
744 Hoek HW, Brown AS, Susser E (1998) The Dutch famine and schizophrenia spectrum
745 disorders. Soc Psychiatry Psychiatr Epidemiol 33:373-379.
746 Honsho M, Fujiki Y (2017) Plasmalogen homeostasis - regulation of plasmalogen
747 biosynthesis and its physiological consequence in mammals. FEBS Lett.
748 591:2720-2729.
749 Hossain MS, Abe Y, Ali F, Youssef M, Honsho M, Fujiki Y, Katafuchi T (2017)
750 Reduction of ether-type glycerophospholipids, plasmalogens, by NF-κB signal
751 lLeading to microglial activation. J Neurosci 37:4074-4092.
752 Hossen MA, Nagata Y, Waki M, Ide Y, Takei S, Fukano H, Romero-Perez GA, Tajima S,
753 Yao I, Ohnishi K, Setou M (2015) Decreased level of phosphatidylcholine
754 (16:0/20:4) in multiple myeloma cells compared to plasma cells: a single-cell
755 MALDI-IMS approach. Anal Bioanal Chem 407:5273-5280.
756 Jenkins BT, Hajra AK (1976) Glycerol kinase and dihydroxyacetone kinase in rat brain.
757 J Neurochem 26:377-385.
758 Jinks AL, McGregor IS (1997) Modulation of anxiety-related behaviours following
759 lesions of the prelimbic or infralimbic cortex in the rat. Brain Res 772:181-190.
760 Khashan AS, Abel KM, McNamee R, Pedersen MG, Webb RT, Baker PN, Kenny LC,
761 Mortensen PB (2008) Higher risk of offspring schizophrenia following antenatal
762 maternal exposure to severe adverse life events. Arch Gen Psychiatry
763 65:146-152.
764 Kimura T, Hino K, Kono T, Takano A, Nitta N, Ushio N, Hino S, Takase R, Kudo M,

765 Daigo Y, Morita W, Nakao M, Nakatsukasa M, Tamagawa T, Rafiq AM,
766 Matsumoto A, Otani H, Udagawa J (2018) Maternal undernutrition during early
767 pregnancy inhibits postnatal growth of the tibia in the female offspring of rats by
768 alteration of chondrogenesis. Gen Comp Endocrinol 260:58-66.
769 Kinney DK, Miller AM, Crowley DJ, Huang E, Gerber E (2008) Autism prevalence
770 following prenatal exposure to hurricanes and tropical storms in Louisiana. J
771 Autism Dev Disord 38:481-488.
772 Kirschner DA, Ganser AL (1982) Myelin labeled with mercuric chloride. Asymmetric
773 localization of phosphatidylethanolamine plasmalogen. J Mol Biol 157:635-658.
774 Kundakovic M (2014) Chapter 24 - DNA methyltransferase inhibitors and psychiatric
775 disorders A2 - Peedicayil, Jacob. In: Epigenetics in Psychiatry (Grayson DR,
776 Avramopoulos D, eds), pp497-514. Boston: Academic Press.
777 Kundakovic M, Jaric I (2017) The epigenetic link between prenatal adverse
778 environments and neurodevelopmental disorders. Genes 8:104.
779 Liao F, Yoon H, Kim J (2017) Apolipoprotein E metabolism and functions in brain and
780 its role in Alzheimer's disease. Curr Opin Lipidol 28:60-67.
781 Liu YL, Fann CS, Liu CM, Chen WJ, Wu JY, Hung SI, Chen CH, Jou YS, Liu SK,
782 Hwang TJ, Hsieh MH, Ouyang WC, Chan HY, Chen JJ, Yang WC, Lin CY, Lee
783 SF, Hwu HG (2006) A single nucleotide polymorphism fine mapping study of
784 chromosome 1q42.1 reveals the vulnerability genes for schizophrenia, GNPAT
785 and DISC1: association with impairment of sustained attention. Biol Psychiatry
786 60:554-562.
787 Markham JA, Koenig JI (2011) Prenatal stress: role in psychotic and depressive
788 diseases. Psychopharmacology 214:89-106.

789 Marques AH, Bjørke-Monsen AL, Teixeira AL, Silverman MN (2015) Maternal stress,
790 nutrition and physical activity: Impact on immune function, CNS development
791 and psychopathology. Brain Res 1617:28-46.
792 Matrisciano F, Tueting P, Maccari S, Nicoletti F, Guidotti A (2012) Pharmacological
793 activation of group-II metabotropic glutamate receptors corrects a
794 schizophrenia-like phenotype induced by prenatal stress in mice.
795 Neuropsychopharmacology 37:929-938.
796 Matrisciano F, Tueting P, Dalal I, Kadriu B, Grayson DR, Davis JM, Nicoletti F,
797 Guidotti A (2013) Epigenetic modifications of GABAergic interneurons are
798 associated with the schizophrenia-like phenotype induced by prenatal stress in
799 mice. Neuropharmacology 68:184-194.
800 McKenna M, Dienel G, Sonnewald U, Waagepetersen H, Schousboe A (2011) Energy
801 metabolism of the brain. In: Basic neurochemistry: principles of molecular,
802 cellular, and medical neurobiology (Brady S, Siegel G, Albers RW, Price D, eds),
803 pp 200-231: Elsevier Science.
804 Moreno M, Economidou D, Mar AC, López-Granero C, Caprioli D, Theobald DE,
805 Fernando A, Newman AH, Robbins TW, Dalley JW (2013) Divergent effects of
806 $D_{2/3}$ receptor activation in the nucleus accumbens core and shell on impulsivity
807 and locomotor activity in high and low impulsive rats. Psychopharmacology
808 228:19-30.
809 Morita SY, Deharu Y, Takata E, Nakano M, Handa T (2008) Cytotoxicity of lipid-free
810 apolipoprotein B. Biochim Biophys Acta 1778:2594-2603.
811 Nguyen LN, Ma D, Shui G, Wong P, Cazenave-Gassiot A, Zhang X, Wenk MR, Goh EL,
812 Silver DL (2014) Mfsd2a is a transporter for the essential omega-3 fatty acid

docosahexaenoic acid. Nature 509:503-506.

Nishiumi S, Kobayashi T, Ikeda A, Yoshie T, Kibi M, Izumi Y, Okuno T, Hayashi N, Kawano S, Takenawa T, Azuma T, Yoshida M (2012) A novel serum metabolomics-based diagnostic approach for colorectal cancer. PLoS One 7:e40459.

Roseboom TJ, van der Meulen JH, Ravelli AC, Osmond C, Barker DJ, Bleker OP (2001) Effects of prenatal exposure to the Dutch famine on adult disease in later life: an overview. Mol Cell Endocrinol 185:93-98.

Sasaki A, de Vega WC, St-Cyr S, Pan P, McGowan PO (2013) Perinatal high fat diet alters glucocorticoid signaling and anxiety behavior in adulthood. Neuroscience 240:1-12.

Schoenwolf GC, Bleyl SB, Brauer PR, Francis-West PH, Larsen WJ (2015) Larsen's human embryology.

Scofield MD, Heinsbroek JA, Gipson CD, Kupchik YM, Spencer S, Smith AC, Roberts-Wolfe D, Kalivas PW (2016) The nucleus accumbens: mechanisms of addiction across drug classes reflect the importance of glutamate homeostasis. Pharmacol Rev 68:816-871.

Spencer RC, Devilbiss DM, Berridge CW (2015) The cognition-enhancing effects of psychostimulants involve direct action in the prefrontal cortex. Biol Psychiatry 77:940-950.

Sugiyama E, Masaki N, Matsushita S, Setou M (2015) Ammonium sulfate improves dDetection of hydrophilic quaternary ammonium compounds through decreased ion suppression in matrix-assisted laser desorption/ionization imaging mass spectrometry. Anal Chem 87:11176-11181.

837 Suzuki K, Sugihara G, Ouchi Y, Nakamura K, Futatsubashi M, Takebayashi K,
838 Yoshihara Y, Omata K, Matsumoto K, Tsuchiya KJ, Iwata Y, Tsujii M, Sugiyama
839 T, Mori N (2013) Microglial activation in young adults with autism spectrum
840 disorder. JAMA Psychiatry 70:49-58.
841 Taguchi R, Ishikawa M (2010) Precise and global identification of phospholipid
842 molecular species by an Orbitrap mass spectrometer and automated search
843 engine Lipid Search. J Chromatogr A 1217:4229-4239.
844 Tsugawa H, Bamba T, Shinohara M, Nishiumi S, Yoshida M, Fukusaki E (2011)
845 Practical non-targeted gas chromatography/mass spectrometry-based
846 metabolomics platform for metabolic phenotype analysis. J Biosci Bioeng
847 112:292-298.
848 Vance JE (2015) Phospholipid synthesis and transport in mammalian cells. Traffic
849 16:1-18.
850 Vieira DB, Gamarra LF (2016) Getting into the brain: liposome-based strategies for
851 effective drug delivery across the blood-brain barrier. Int J Nanomedicine
852 11:5381-5414.
853 Werling DM, Geschwind DH (2013) Sex differences in autism spectrum disorders. Curr
854 Opin Neurol 26:146-153.
855 Wong H, Hoeffer C (2018) Maternal IL-17A in autism. Exp Neurol 299:228-240.
856 Wu ZM, Bralten J, Cao QJ, Hoogman M, Zwiers MP, An L, Sun L, Yang L, Zang YF,
857 Franke B, Wang YF (2017) White Matter Microstructural Alterations in Children
858 with ADHD: Categorical and Dimensional Perspectives.
859 Neuropsychopharmacology 42:572-580.
860 Yeagle PL (2016) Chapter 3 - Biogenesis of membrane lLipids. In: The

Membranes of Cells (3rd Edition), pp 57-71. Boston: Academic Press.

Yu TW et al. (2013) Using whole-exome sequencing to identify inherited causes of autism. Neuron 77:259-273.

Zemski Berry KA, Gordon WC, Murphy RC, Bazan NG (2014) Spatial organization of lipids in the human retina and optic nerve by MALDI imaging mass spectrometry. J Lipid Res 55:504-515.

Zhu Y, Yang D, Ji W, Huang T, Xue L, Jiang X, Chen L, Wang F (2016) The relationship between neurocircuitry dysfunctions and attention deficit hyperactivity disorder: a review. Biomed Res Int 2016:3821579.

Figure legends

Fig. 1 Study design and behavior of rat offspring subjected to prenatal undernutrition. (A) The experimental schedule is shown. The daily food intake was restricted from GD5.5 to GD10.5 or from the day of blastocyst implantation to the day just before the closure of the neural tube. (B–F) Behavioral tests at 8 weeks of age: male rat offspring exhibited hyperactivity in the LPD (n = 18), 50F (n = 13), and 40F (n = 17) groups compared with the offspring in the AL group (n = 32). (G–K) Behavioral tests at 12 weeks of age: behavioral disturbances continued at 12 weeks of age in the LPD (n = 19) and 50F (n = 14) offspring compared with the AL offspring (n = 18). The statistical analysis was conducted using one-way ANOVA with Dunnett's test. *$p < 0.05$, **$p < 0.01$, *** $p < 0.001$; A1: the area of the center region, A2: the area of the peripheral region.

885 Fig. 2 Preparation of the brain sections for MALDI-IMS (A) Rat brain sections were
886 aligned between adjacent mouse brain sections (references). (B) Peak intensity of each
887 phospholipid was corrected using the average peak intensity of the same phospholipid
888 of the mouse reference sections.
889
890 Fig. 3 Metabolome profiling of the plasma and CSF, and the observation of microglia in
891 the PFC. (A) 2-aminoethanol and glycerol increased in the rat offspring exposed to
892 prenatal undernutrition (plasma: n = 7 in AL and n =6 in 40F; CSF: n = 7 in AL and n =
893 5 in 40F) (See also Figure 3-1). (B) The dotted area, which was the middle third of the
894 box area, was examined. (C) Microglial cell activation in the PFC Iba1-positive
895 microglia (green), CD11b-positive cells (red), and activated microglia (yellow) are
896 shown in the PFC of the offspring of the AL and 40F groups. Scale bar, 20 mm. (D) The
897 densities of microglia and activated microglia were not increased in the PFC of 40F (n =
898 8) offspring compared with AL (n = 8) offspring. (E) The ratio of the number of
899 activated microglia to the total number of microglia was not altered by prenatal
900 undernutrition. *$p < 0.05$, **$p < 0.01$, Student's *t*-test.
901
902 Fig. 4 Biosynthetic pathway of plasmalogens and diacyl phospholipids. The enzymes
903 related to phospholipid synthesis, with intermediates, are shown. The genes indicated
904 by underlined bold italic characters were activated. Abbreviations of the
905 genes are noted as follows: *Hk:Hexokinase, GPI:Glucose-6-phosphate isomerase,*
906 *Pfk:Phosphofructokinase, aldoiase:Fructose-bisphosphate aldoiase,*
907 *Gpd:Glycerol-3-phosphate dehydrogenase, Far:fatty acyl-CoA reductase, Gk:Glycerol*
908 *kinase, Gnpat:Glyceronephosphate O-acyltransferase, Agps:Alkylglycerone phosphate*

synthase, ADHAPAR:Alkyl/acyl-glycerophosphate acyltransferase, Plpp:Phosphatidic acid phosphatase, Cept:Choline/ethanolamine phosphotransferase, Plasmenylethanolamine desaturase, Ept:Ethanolamine phosphotransferase, Chpt:Choline phosphotransferase, Gpat:Glycerol-3-phosphate acyltransferase, Lpcat: LysoPA-acyltransferase, Chk:choline kinase, Etnk:Ethanolamine kinase, Pemt:Phosphoethanolamine N-methyltransferase, Pcyt:Phospate cytidyltransferase, Pisd:Phosphatidylserine decarboxylase, Ptdss:Phosphatidylserine synthase, CDS:CDP-diacylglycerol synthase, Sgms:Sphingomyelin synthase, Smpd:Sphingomyelin phosphodiesterase, Pis:Phosphatidylinositol synthase, Pgps:Phosphatidylglycerophosphate synthase, Cls:Cardiolipin synthase, PE:Phosphatidylethanolamine, PC: Phosphatidylcholine, PS: Phosphatidylserine, PI: Phosphatidylinositol, CL:Cardiolipin, PG, Phosphatidylglycerol, SM:Sphingomyelin.

Fig. 5 Gene expression of the enzymes related to phospholipid synthesis and phospholipid composition of the rat brain. (A) The area examined by gene expression analysis (B) The ratios of the expression levels of the enzymes in the synthetic pathway of plasmalogens and diacyl phospholipids in the PFC, NAcc, and CPu for the 40F-group offspring (n = 8) were compared with those for the AL-group offspring (n = 8) (See Figure 5-1). (C) The area examined by MALDI-IMS. The dotted areas were examined in the PFC, NAcc, and CPu. In a section of the PFC, the dotted area is the middle third of the box area indicated by the solid line. Signal intensity was indicated by color. (D) The ratios of peak intensities of phospholipids of 40F offspring (n = 7) to those of AL offspring (n = 7) are shown (See Figure 5-2). (E) The peaks of product ions by collision-induced dissociation of m/z 774.5 in MALDI tandem mass spectrometry.

933 *$p < 0.05$, **$p < 0.01$, Student's *t*-test.

934

935 Fig. 6 Behavioral tests and phospholipid composition in the brain of the rats injected
936 with PE. (A) The experimental schedule of the liposome injection at 14 weeks of age.
937 Changes in the behavior of rats by using the open-field test after (B) PE (18:0p-22:6)
938 (PEL: n = 6, CL: n = 7), or (C) POPE injection (POPEL: n = 5, CL: n = 5, saline: n = 4)
939 were examined by ANCOVA. Similarly, behavioral changes evaluated according to the
940 elevated plus maze test after (D) PE (18:0p-22:6) (PEL: n = 6, CL: n = 6), or (E) POPE
941 injection (POPEL: n = 5, CL: n = 5, saline: n = 4) were examined. (F) The ratios of peak
942 intensities of phospholipids in the brains of PEL-injected rats (n = 4) significantly
943 increased compared with those of CL-injected rats (n = 4) using Student's *t*-test (See
944 also Figure 6-1). The increased ratio of peak intensity of PE (18:0p-22:6) in the PFC of
945 PEL-injected rats was verified in an additional experiment (See Figure 6-2). (G) The
946 ratio of PE (18:0p-22:6) to total lipids in the blood cells was compared among CL PEL
947 and saline groups using one-way ANOVA with Tukey's HSD test. *$p < 0.05$, ns: not
948 significant.

949

950 Fig. 3-1 Metabolomics of the plasma and CSF in male offspring aged 9 weeks. All data
951 identified in this study are shown. The peak height of a particular ion for each
952 metabolite was normalized to the peak height of the specified ion of 2-isopropylmalic
953 acid in metabolic profiling. *$p < 0.05$, Student's *t*-test, ND: not detected.

954

955 Fig. 5-1 Gene expression profiles in male offspring aged 9 weeks. Comparative Cq
956 values of the target genes normalized to B2m are shown. *$p < 0.05$, Student's *t*-test,

957 ND: not detected, NE: not examined.

958

959 Fig. 5-2 Change in phospholipid composition in PFC, NAcc, and CPu by undernutrition.
960 All data examined in this study are shown. *$p < 0.05$, Student's *t*-test.

961

962 Fig. 6-1 Phospholipid composition in PFC, NAcc, and CPu of the rats injected with
963 liposomes. All data examined in this study are shown. *$p < 0.05$, Student's *t*-test.

964

965 Fig. 6-2 Phospholipid composition in PFC of the rats injected with liposomes in the
966 verification experiment. To verify whether PE (18:0p-22:6) was elevated in the brain
967 following PE injection, phospholipid composition was analyzed in PFC sections of male
968 rats in the PEL (n = 5) and CL (n = 5) after two shots of PE (18:0p-22:6) using the
969 method described in the Materials and Methods section. This experiment was conducted
970 separately from the PEL injection study in Fig. 6F. PE (18:0p-22:6) significantly
971 increased in the PFC of the rats injected with PEL liposomes ($p = 0.032$, d = 1.83). *p
972 < 0.05, Student's *t*-test.

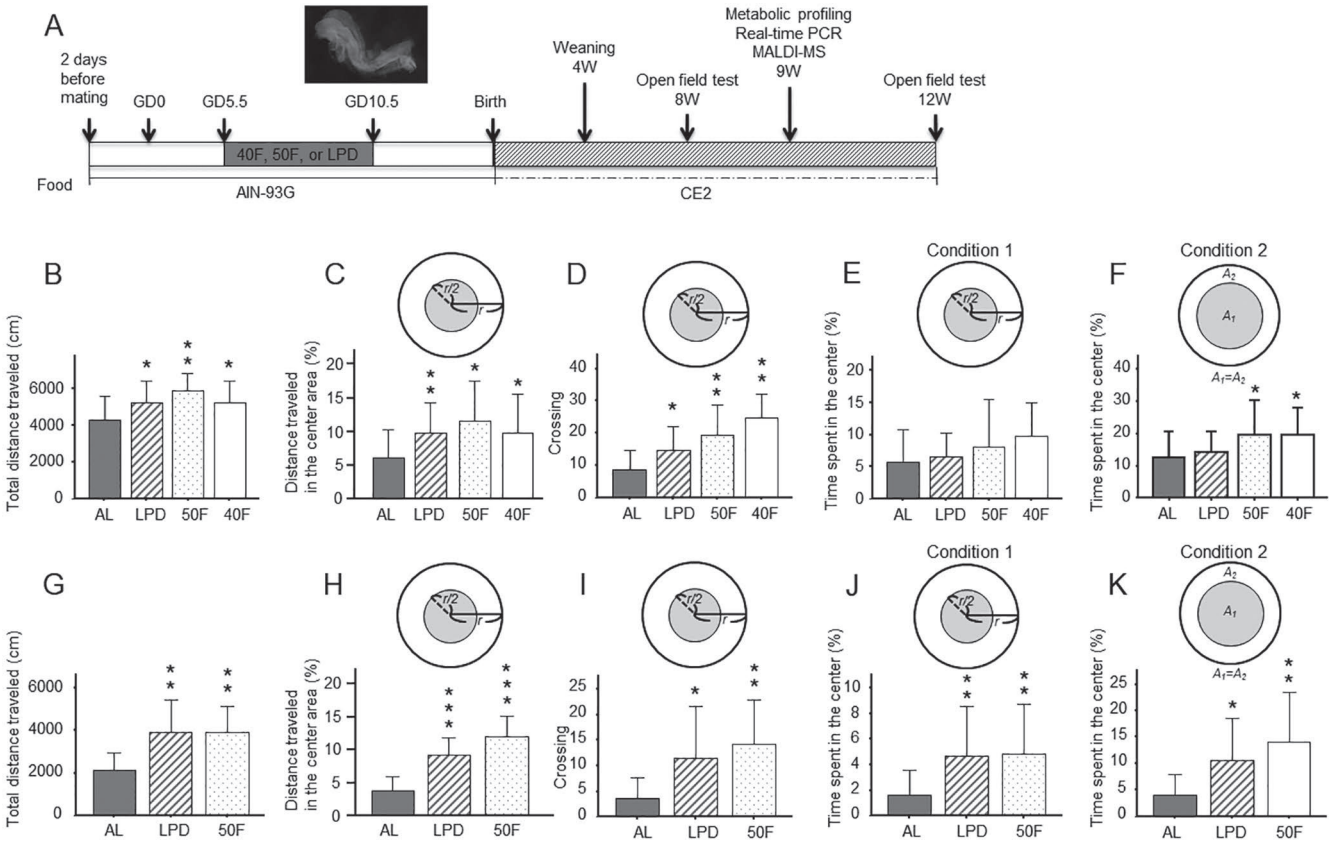

A

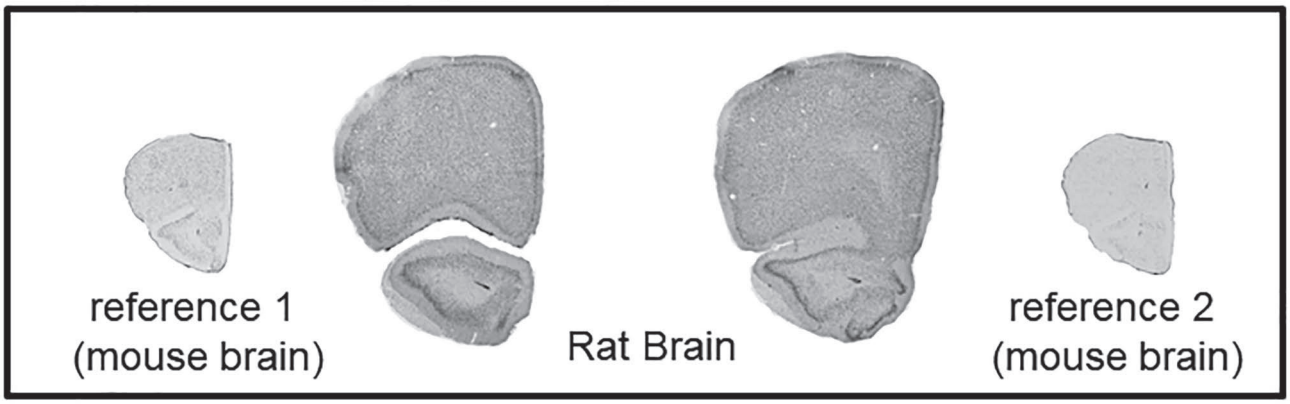

B

$$\text{Peak intensity} = \frac{\text{Peak intensity of phospholipid X in the rat brain}}{\text{Average raw peak intensity of phospholipid X in references 1 and 2}}$$

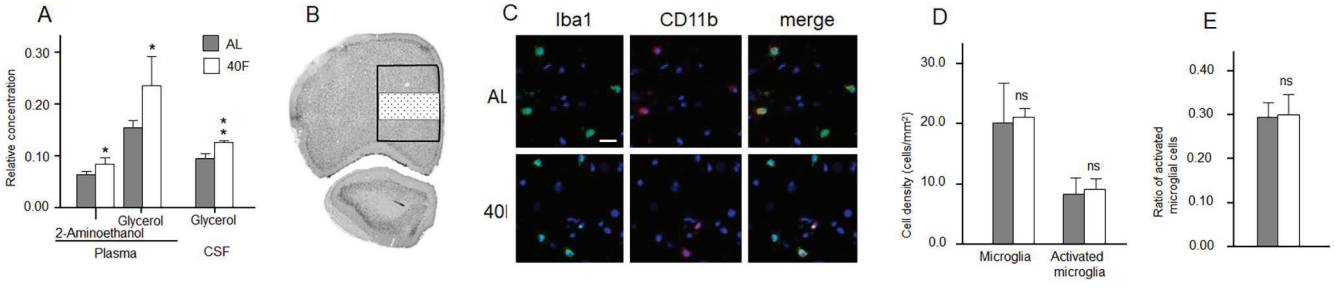

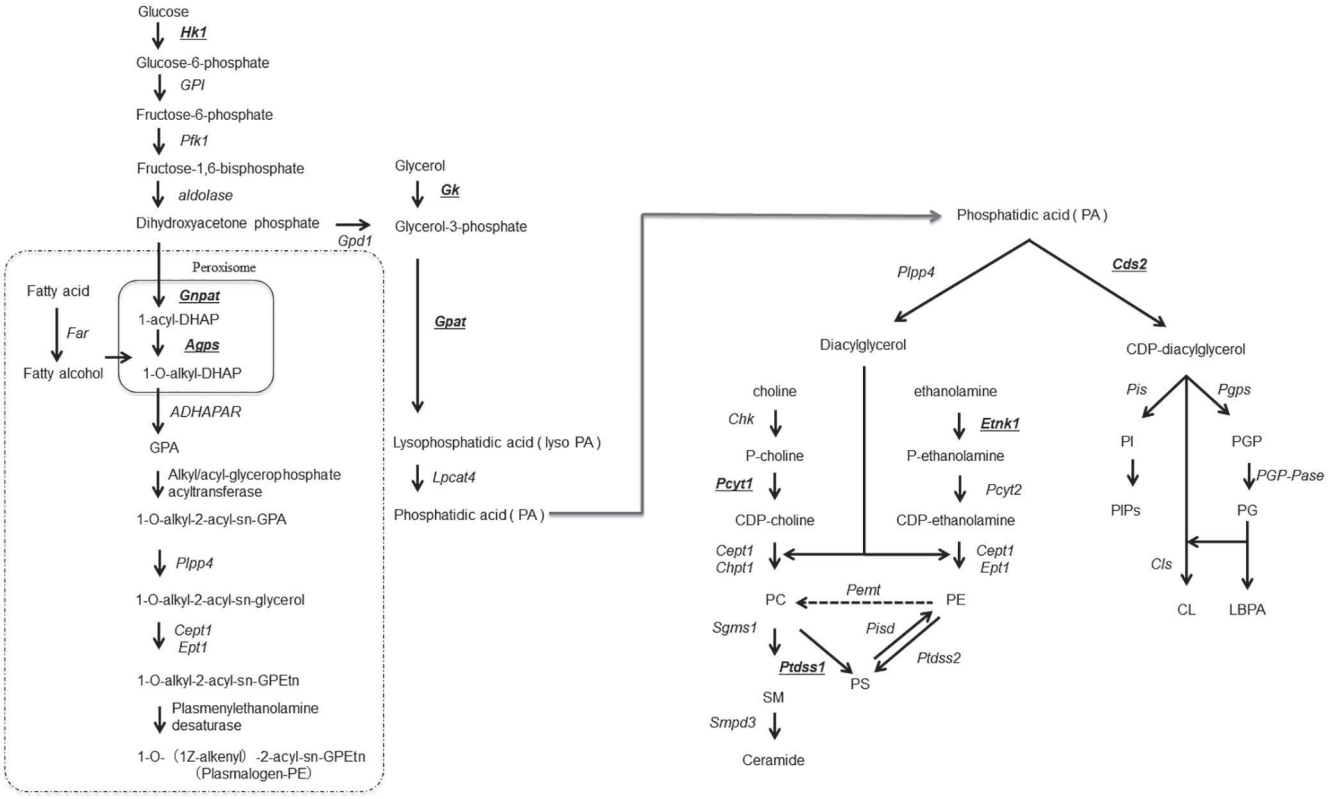

Synthetic pathway of plasmalogens

Synthetic pathway of diacyl phospholipids

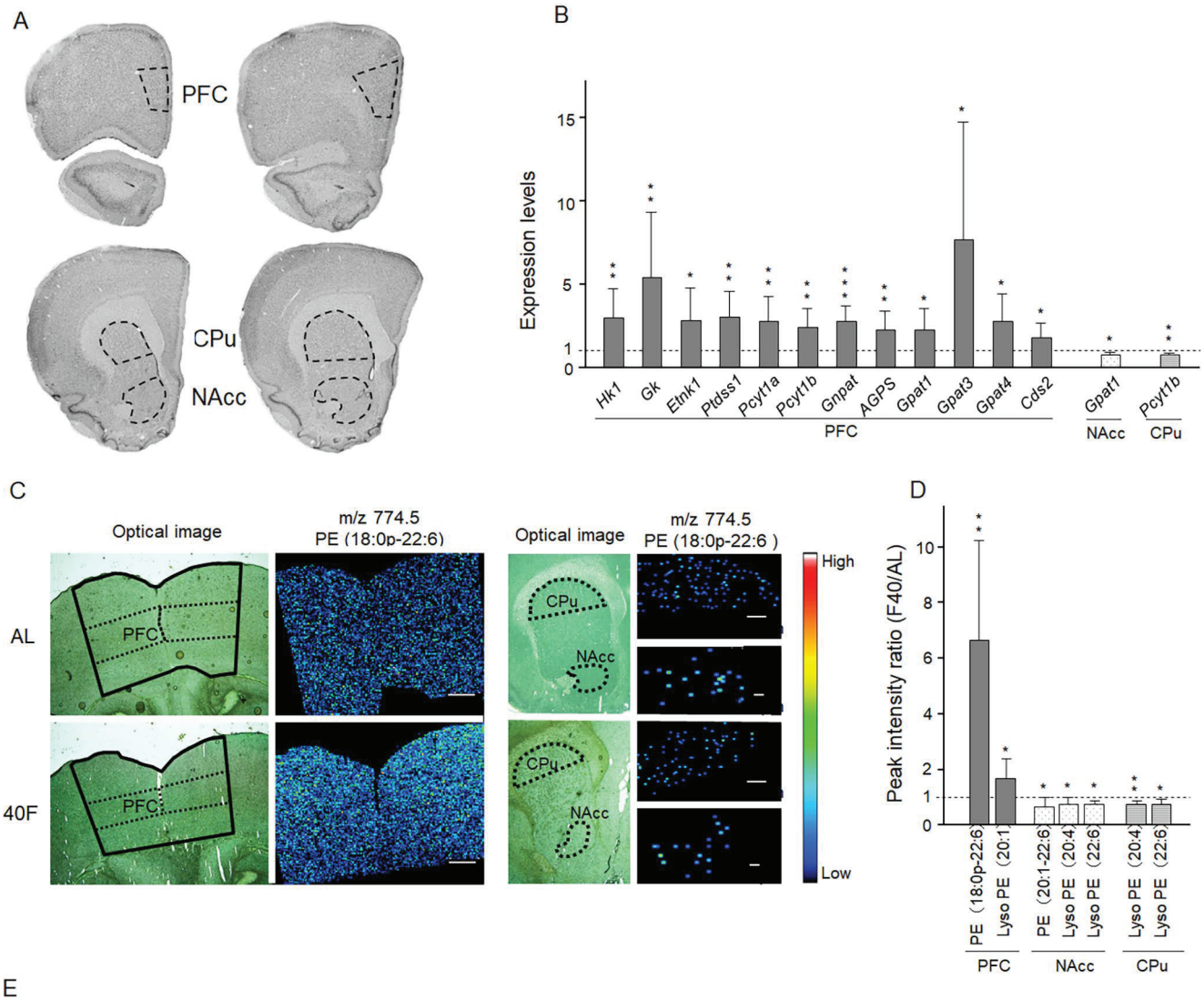

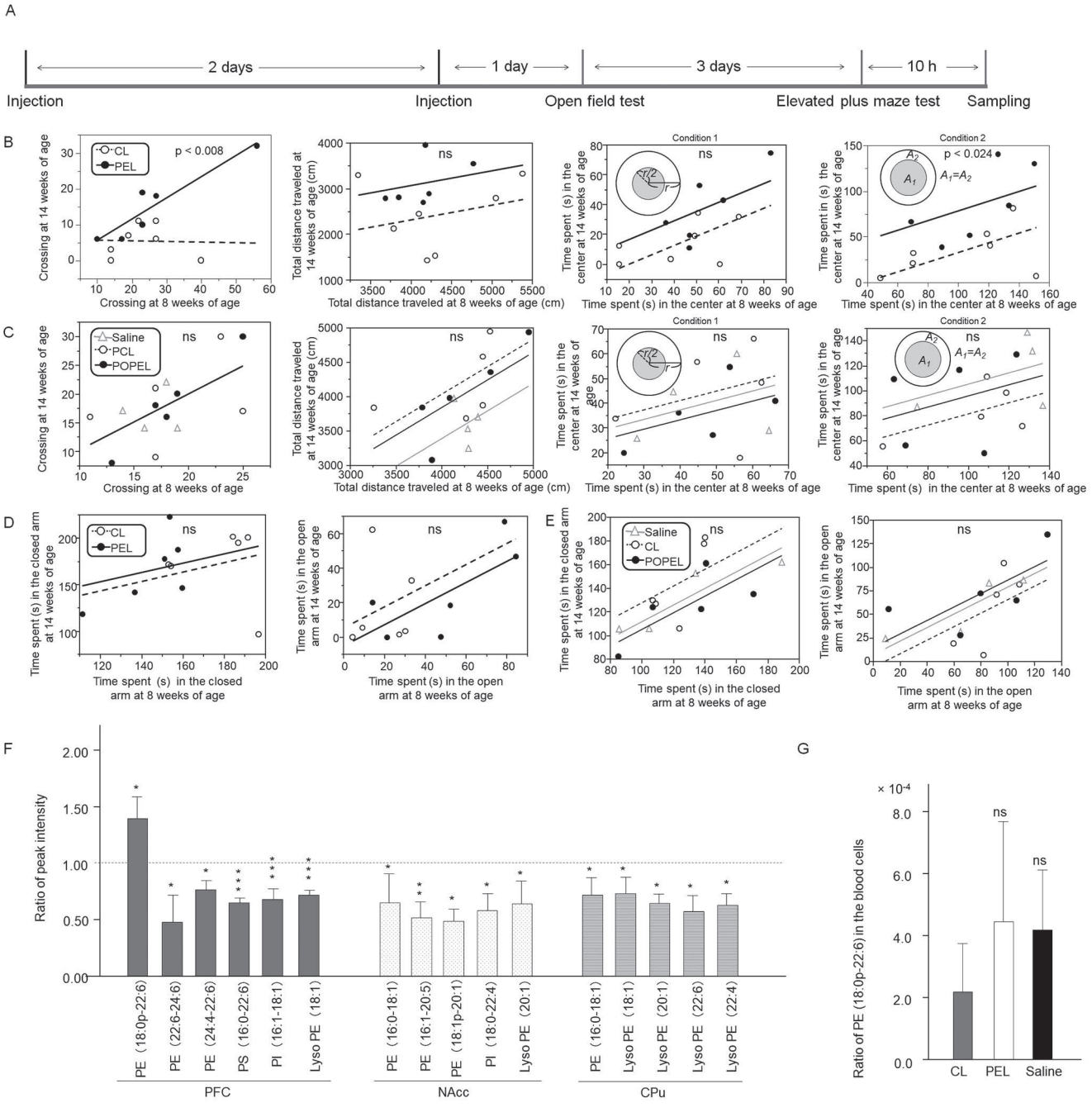

Table 1 Primer sequences for real-time PCR

Gene symbol	Forward primer sequence (5'>3')	Reverse primer sequence (5'>3')	Acc. number	Amplicon size (bp)
Agps	TCCTACTCACAAGACGCAGA	AGGAATCCGCTCAAACATCC	NM_053350.2	99
Apoe	CCGCAACGAGGTAAACACCA	ATCATCCGCATCCCGCATC	NM_001270684.1	109
Aqp9	AGCCGGATAGCGAAGGAGA	AGTGATGATCCCGCCAAAAC	NM_022960.2	120
B2M	CGAGACCGATGTATATGCTTGC	GTCCAGATGATTCAGAGCTCCA	NM_012512.2	114
Cds2	CCACCGGTTCATCTCCTTTAC	GCGTTACGACAATAAGCAAGG	NM_053643.1	134
Cept1	AGTCTTCTACTGCCCTACAGC	TTCTTCTGGCCTGTTTCCCG	NM_001007.1	119
Chka	CAACAACTGCACAAGTTCCTC	CTCTTGGCCTTCCAACAATAAG	NM_017127.1	144
Chkb	GTCCACTAGCCTTCCCCAGA	CCTGGATGTCATTGTGGCAG	NM_017177.1	125
Etnk1	AGCTCGTCAGCTTGCTAAAATC	CTTCATCAGCAAATCCTGTGGG	NM_001107894.1	122
Far1	CCCTTGCAGATCTCGTTCCT	AGGATTAGTGCTGCCTGTTGT	XM_006230020.3	125
Gk	GAAACTTCGTTGGCTCCTCG	GAACACCGCCATTGATTCCC	NM_024381.2	128
Gnpat	GTGTGTGTGAATGAAGAAGGCA	GGACAAAGGACAGCATGAGGA	NM_053410.1	115
Gpat1	GGCAACAACCTCAACATCCC	TTGCGTCCATCTGGAGTTTC	NM_017274.1	98
Gpat3	ACACTGGTTGGCCAGCTTC	AGACAGGGAGCGAACACAGA	XM_008770021.2	96
Gpat4	GCTCAAACCAGACATGGGGG	TTGCTAACCATACGTCGCCC	NM_001047849.1	141
Gpd1	AGCATCCTCCAACACAAGGG	GCAGCAGATGAACTCACCCA	NM_022215.2	102
Hk1	ACCCGGAAATTCGTTCCTCC	TCTTTTGTCCGGAGCATCCC	NM_012734.1	80
iPLA2	CCCATCCACACAGCCATGAA	AGAAGCATTCGGGCCATCTC	XM_006242004.2	149
Lpcat4	GGAGCAGCTTCAGGAACCAA	CGAAGGAAGCCAAGCAGGAA	NM_001106494.1	102
Mfsd2a	GCTTCTGCATCAGCAAGTCC	GGGAAGTCAGGCACAAACCA	NM_001106683.1	118
Mfsd3	GGTGCTTCTGCCTCAGATTT	GCACTGACCTCAACAGCTTC	NM_001024908.1	142
Plpp4	TGCTTTCCAGATGGGGTGATG	CAACTTGCCAGCCAGGTAGAA	NM_001191631.1	150
Pcyt1a	ATCCCCTACTCTTCGGCAGG	GGACAATGCGGGTGATGAGG	NM_078622.2	121
Pcyt1b	TCATCTCGGGGTTCTGATGAC	ACGGACAATTCTGGTGATGATG	NM_173151.1	114
Pcyt2	ATGTGGCTGGTGCCTTTGA	AAAGTGTAGGCCCGCGATGA	NM_053568.1	104
Pemt	GTACTGGGGAAGTACAGCCAAC	CTTCAAACAGGAGAGCAACCAC	NM_013003.1	116
Pfkp	AAGTACCTGGAGCACCTCTCT	TGTATATTCCCATGCGCACCA	NM_206847.1	115
Pisd	ATGTGGGCTCTATCCGCATC	TGGGAATGCCCTCCTTGTTG	XM_002725000.4	120
Ptdss1	TATGGGCTCTGCTGGACAATC	CCACCACCATTACACAACAGG	NM_001012133.1	131
Ptdss2	AACCCCTCAGGATACAGCCTAC	CTAACACACAGCCAAAACCGC	NM_001106316.1	144
Smpd3	TGTCTCAACAGCGGTCTCTTC	GTACAGGCGATGTACCCAACA	NM_053605.1	176
Sgms1	ATGCTAACGCTCACCTACCTG	GTGTAGTGGTCATGCGCTAA	NM_181386.2	128

Table 2 Allocation of experimental groups

Treatment	Experiment	Age (weeks)	
Under nutrition	Open-field test	8	AL, 40F, 50F, LPD
	Open-field test	12	AL, 50F, LPD
	Metabolic profiling (plasma, CSF)	9	AL, 40F
	Counting microglial cells (PFC)	9	AL, 40F
	Gene expression (PFC, NAcc, CPu)	9	AL, 40F
	MALDI-IMS (PFC, NAcc, CPu)	9	AL, 40F
Liposome injection	Open-field test	8 and 14	CL, PEL, POPEL, saline
	Elevated plus maze test	8 and 14	CL, PEL, POPEL, saline
	MALDI-IMS (PFC, NAcc, CPu, blood cells)	14	CL, PEL

AL: *ad libitum* group, 40F or 50F: the group fed 40% or 50% of the daily food intake of the AL, respectively, LPD: low protein diet group

CL, PEL, POPEL, or saline: the group injected with control, PE (18:0p-22:6), or POPE liposome, or saline

Table 3 Body weight of the offspring

Group	Body weight (g)	
	9 weeks of age	12 weeks of age
AL	271.4 ± 26.5 (n = 32)	315.5 ± 26.0 (n = 18)
50F	248.7 ± 20.6* (n = 18)	317.7 ± 26.2 (n = 18)
40F	267.8 ± 28.8 (n = 18)	Not measured
LPD	250.4 ± 17.3* (n = 19)	325.7 ± 18.5 (n = 19)

Values are means ± SD, *$p < 0.05$ vs AL (One-way ANOVA with Dunnett's test)

Table 4 Change in amounts of DHA- or AA-containing phospholipids in PFC, NAcc, and CPu by undernutrition

Phospholipid	sn1_sn2	PFC		NAcc		CPu	
		AL	40F	AL	40F	AL	40F
		Mean ± SD	Mean ± SD	Mean ± SD	Mean ± SD	Mean ± SD	Mean ± SD
Lyso PE_AA	20:4 (Acyl)	3.86 ± 1.20	6.30 ± 2.70	3.60 ± 0.67	2.60 ± 0.77*	3.76 ± 0.57	2.75 ± 0.39*
Lyso PE_DHA	22:6 (Acyl)	2.54 ± 0.84	3.67 ± 1.17	2.23 ± 0.46	1.70 ± 0.26*	2.48 ± 0.33	1.92 ± 0.38*
PE_AA_Pls	16:0p-20:4 (Alkenyl_acyl)	2.83 ± 0.95	3.97 ± 1.70	4.52 ± 1.46	4.52 ± 0.86	3.27 ± 0.74	3.46 ± 0.76
	18:1p-20:4 (Alkenyl_acyl)	2.07 ± 0.72	2.48 ± 1.03	2.15 ± 0.41	2.02 ± 0.43	1.94 ± 0.27	1.90 ± 0.42
PE_AA_Acyl	18:1-20:4 (Alkyl_acyl)	2.71 ± 0.86	3.39 ± 1.31	3.65 ± 0.82	3.38 ± 0.63	2.89 ± 0.50	3.00 ± 0.62
	18:0-20:4 (Alkyl_acyl)	2.95 ± 0.73	4.29 ± 1.87	3.83 ± 0.95	3.21 ± 0.72	3.14 ± 0.76	2.97 ± 0.59
	18:2-20:4 (Diacyl)	1.37 ± 0.47	1.67 ± 0.67	1.21 ± 0.22	1.19 ± 0.26	1.18 ± 0.17	1.19 ± 0.27
	18:1-20:4 (Diacyl)	1.67 ± 0.54	2.10 ± 0.88	1.64 ± 0.31	1.45 ± 0.26	1.67 ± 0.20	1.49 ± 0.27
	18:0-20:4 (Diacyl)	1.84 ± 0.56	2.35 ± 0.96	2.38 ± 0.32	2.11 ± 0.42	1.74 ± 0.19	1.72 ± 0.40
PE_DHA_Pls	18:0p-22:6 (Alkenyl_acyl)	1.41 ± 0.43	9.39 ± 4.62*	1.74 ± 0.32	1.67 ± 0.30	1.79 ± 0.28	1.75 ± 0.32
	18:1p-22:6 (Alkenyl_acyl)	1.30 ± 0.36	1.63 ± 0.65	1.28 ± 0.24	1.16 ± 0.20	1.34 ± 0.26	1.26 ± 0.19
	20:1p-22:6 (Alkenyl_acyl)	3.11 ± 1.38	3.46 ± 0.85	2.09 ± 0.69	1.77 ± 0.82	2.48 ± 1.14	2.13 ± 0.49
PE_DHA_Acyl	16:1-22:6 (Diacyl)	1.36 ± 0.38	1.64 ± 0.84	1.80 ± 0.41	1.55 ± 0.26	1.86 ± 0.24	1.66 ± 0.20
	18:0-22:6 (Alkyl_acyl)	1.67 ± 0.46	2.19 ± 0.92	1.94 ± 0.45	1.70 ± 0.34	1.93 ± 0.35	1.93 ± 0.41
	18:2-22:6 (Diacyl)	1.75 ± 0.66	2.27 ± 1.09	1.56 ± 0.29	1.37 ± 0.31	1.93 ± 0.32	1.73 ± 0.42
	18:0-22:6 (Diacyl)	1.31 ± 0.42	1.67 ± 0.63	1.46 ± 0.28	1.46 ± 0.31	1.44 ± 0.22	1.48 ± 0.31
	20:1-22:6 (Diacyl)	3.00 ± 1.17	3.65 ± 1.96	2.72 ± 0.71	1.76 ± 0.77*	3.08 ± 0.91	2.69 ± 1.20
	20:0-22:6 (Diacyl)	2.16 ± 0.85	3.42 ± 1.71	3.28 ± 1.08	2.58 ± 1.73	4.47 ± 1.45	3.74 ± 2.08
	22:6-22:6 (Diacyl)	1.86 ± 0.72	2.35 ± 0.98	1.87 ± 0.35	1.76 ± 0.40	1.74 ± 0.29	1.73 ± 0.39
	22:6-24:6 (Diacyl)	2.74 ± 2.55	2.90 ± 0.55	1.41 ± 0.40	1.05 ± 0.28	3.52 ± 1.30	3.23 ± 0.81

	24:4-22:6 (Diacyl)	2.97 ± 1.20	3.55 ± 1.41	1.74 ± 0.58	2.01 ± 1.46	2.24 ± 0.80	2.49 ± 1.23
PS_AA_Acyl	18:1-20:4 (Diacyl)	2.00 ± 0.63	2.94 ± 1.50	3.50 ± 1.28	3.16 ± 0.76	6.01 ± 1.91	6.38 ± 1.87
PS_DHA_Acyl	16:0-22:6 (Diacyl)	1.46 ± 0.47	2.39 ± 1.13	3.91 ± 0.94	3.35 ± 0.68	7.26 ± 1.62	7.21 ± 1.56
	18:1-22:6 (Diacyl)	2.64 ± 0.97	3.12 ± 1.57	1.73 ± 0.63	1.63 ± 0.43	2.14 ± 0.46	1.88 ± 0.38
	20:0-22:6 (Diacyl)	2.11 ± 0.67	4.29 ± 2.46	2.12 ± 0.92	1.89 ± 0.54	2.72 ± 1.02	2.47 ± 0.50
	22:4-22:6 (Diacyl)	2.10 ± 1.19	3.56 ± 2.64	1.56 ± 0.22	1.56 ± 0.44	1.91 ± 0.29	1.77 ± 0.45
PS_AA_DHA	20:4-22:6 (Diacyl)	2.09 ± 0.77	2.52 ± 1.08	2.02 ± 0.57	1.82 ± 0.44	2.01 ± 0.69	2.16 ± 0.77
Lyso PI_AA	20:4 (Acyl)	3.40 ± 1.67	4.53 ± 2.83	4.39 ± 1.03	4.06 ± 2.43	4.22 ± 0.64	3.99 ± 2.32
PI_AA_Acyl	16:1-20:4 (Diacyl)	5.79 ± 8.33	4.14 ± 2.30	1.92 ± 0.39	1.87 ± 0.50	2.44 ± 0.66	2.21 ± 0.22
	16:0-20:4 (Diacyl)	2.07 ± 0.84	2.38 ± 1.07	4.77 ± 7.19	1.44 ± 0.49	4.67 ± 6.92	1.52 ± 0.50
	18:0-20:4 (Alkyl_acyl)	2.83 ± 1.19	2.67 ± 1.19	1.98 ± 0.56	1.82 ± 0.28	2.27 ± 0.53	2.11 ± 0.30
	18:1-20:4 (Diacyl)	1.89 ± 0.77	2.23 ± 1.01	1.70 ± 0.36	1.42 ± 0.49	1.59 ± 0.32	1.43 ± 0.42
	18:0-20:4 (Diacyl)	2.28 ± 0.83	2.79 ± 1.19	2.71 ± 0.77	2.66 ± 0.78	2.80 ± 0.39	2.69 ± 0.75
PI_DHA_Acyl	18:0-22:6 (Diacyl)	2.22 ± 0.87	2.82 ± 1.80	1.17 ± 0.33	1.17 ± 0.35	1.64 ± 0.33	1.34 ± 0.56

*$p < 0.05$

Table 5 Change in amounts of DHA- or AA-containing phospholipids in PFC, NAcc, and CPu of the rats injected with liposomes

Phospholipid	sn1_sn2	PFC		NAcc		CPu	
		PEL	CL	PEL	CL	PEL	CL
		Mean ± SD	Mean ± SD	Mean ± SD	Mean ± SD	Mean ± SD	Mean ± SD
Lyso PE_AA	20:4 (Acyl)	1.94 ± 0.21	2.17 ± 0.24	1.44 ± 0.79	2.15 ± 0.88	1.31 ± 0.15	1.87 ± 0.58
Lyso PE_DHA	22:6 (Acyl)	1.29 ± 0.23	1.55 ± 0.09	1.00 ± 0.45	1.24 ± 0.28	0.88 ± 0.19*	1.55 ± 0.32
PE_AA_Pls	16:0p-20:4 (Alkenyl_acyl)	4.29 ± 0.71	3.66 ± 0.59	3.02 ± 1.03	3.36 ± 0.50	2.19 ± 0.43	2.58 ± 0.62
	18:1p-20:4 (Alkenyl_acyl)	2.25 ± 0.41	2.07 ± 0.32	1.13 ± 0.36	1.36 ± 0.14	1.06 ± 0.24	1.24 ± 0.20
PE_AA_Acyl	18:1-20:4 (Alkyl_acyl)	3.22 ± 0.54	2.70 ± 0.58	2.26 ± 0.73	2.48 ± 0.19	1.88 ± 0.42	2.14 ± 0.36
	18:0-20:4 (Alkyl_acyl)	3.11 ± 0.58	2.28 ± 0.27	2.11 ± 0.65	2.56 ± 0.32	1.82 ± 0.40	2.30 ± 0.29
	18:2-20:4 (Diacyl)	1.87 ± 0.28	1.50 ± 0.24	0.65 ± 0.18	0.73 ± 0.05	0.68 ± 0.13	0.78 ± 0.10
	18:1-20:4 (Diacyl)	1.69 ± 0.39	1.43 ± 0.28	1.02 ± 0.24	1.12 ± 0.17	1.06 ± 0.20	1.19 ± 0.24
	18:0-20:4 (Diacyl)	2.60 ± 0.56	1.97 ± 0.60	1.30 ± 0.35	1.50 ± 0.12	1.07 ± 0.20	1.22 ± 0.16
PE_DHA_Pls	18:0p-22:6 (Alkenyl_acyl)	2.62 ± 0.31*	1.88 ± 0.08	1.06 ± 0.30	1.18 ± 0.05	1.08 ± 0.18	1.18 ± 0.13
	18:1p-22:6 (Alkenyl_acyl)	2.13 ± 0.31	1.99 ± 0.16	0.73 ± 0.23	0.88 ± 0.11	0.84 ± 0.15	1.00 ± 0.15
	20:1p-22:6 (Alkenyl_acyl)	2.99 ± 1.29	2.39 ± 0.22	1.00 ± 0.46	1.04 ± 0.26	1.33 ± 0.30	1.92 ± 0.64
PE_DHA_Acyl	16:1-22:6 (Diacyl)	1.10 ± 0.31	1.03 ± 0.19	0.97 ± 0.27	1.20 ± 0.28	1.26 ± 0.26	1.32 ± 0.27
	18:0-22:6 (Alkyl_acyl)	2.52 ± 0.38	1.87 ± 0.35	0.99 ± 0.31	1.23 ± 0.08	1.17 ± 0.22	1.33 ± 0.15
	18:2-22:6 (Diacyl)	1.29 ± 0.24	1.27 ± 0.20	0.86 ± 0.17	1.08 ± 0.22	1.04 ± 0.34	1.31 ± 0.31
	18:0-22:6 (Diacyl)	1.63 ± 0.32	1.28 ± 0.33	0.82 ± 0.20	0.92 ± 0.10	0.84 ± 0.14	0.93 ± 0.11
	20:1-22:6 (Diacyl)	1.94 ± 0.36	2.05 ± 0.46	0.88 ± 0.31	1.08 ± 0.24	0.92 ± 0.44	1.19 ± 0.39
	20:0-22:6 (Diacyl)	1.85 ± 0.46	2.12 ± 0.21	1.90 ± 1.23	3.23 ± 0.69	2.68 ± 0.40	3.44 ± 0.58
	22:6-22:6 (Diacyl)	1.91 ± 0.41	1.71 ± 0.40	1.05 ± 0.32	1.31 ± 0.13	1.02 ± 0.21	1.20 ± 0.21
	22:6-24:6 (Diacyl)	3.74 ± 1.60*	7.77 ± 0.78	0.61 ± 0.28	0.93 ± 0.59	1.68 ± 0.44	2.23 ± 0.50

	24:4-22:6 (Diacyl)	2.28 ± 0.22*	2.98 ± 0.19	1.08 ± 0.75	1.54 ± 0.20	0.98 ± 0.22	1.43 ± 0.55
PS_AA_Acyl	18:1-20:4 (Diacyl)	1.04 ± 0.14	1.34 ± 0.14	1.73 ± 0.67	2.03 ± 0.25	2.77 ± 0.69	3.32 ± 0.49
PS_DHA_Acyl	16:0-22:6 (Diacyl)	0.60 ± 0.03*	0.91 ± 0.04	1.60 ± 0.62	2.41 ± 1.04	3.56 ± 0.92	4.71 ± 0.98
	18:1-22:6 (Diacyl)	1.80 ± 0.39	1.58 ± 0.18	1.44 ± 0.79	1.23 ± 0.15	1.26 ± 0.41	1.55 ± 0.29
	20:0-22:6 (Diacyl)	1.74 ± 0.29	2.36 ± 0.49	1.00 ± 0.45	1.65 ± 0.45	1.63 ± 0.36	1.69 ± 0.45
	22:4-22:6 (Diacyl)	7.68 ± 2.36	5.82 ± 1.23	3.02 ± 1.03	1.21 ± 0.25	1.16 ± 0.30	1.37 ± 0.22
PS_AA_DHA	20:4-22:6 (Diacyl)	2.33 ± 0.40	2.51 ± 0.32	1.13 ± 0.36	1.54 ± 0.49	1.14 ± 0.34	1.22 ± 0.25
Lyso PI_AA	20:4 (Acyl)	2.80 ± 0.19	3.27 ± 0.32	2.26 ± 0.73	1.33 ± 0.22	1.13 ± 0.31	1.34 ± 0.30
PI_AA_Acyl	16:1-20:4 (Diacyl)	1.88 ± 0.47	1.31 ± 0.08	2.11 ± 0.65	1.71 ± 0.11	1.49 ± 0.42	1.67 ± 0.43
	16:0-20:4 (Diacyl)	2.08 ± 0.43	1.88 ± 0.37	0.65 ± 0.18*	1.32 ± 0.22	0.94 ± 0.21	1.32 ± 0.19
	18:0-20:4 (Alkyl_acyl)	2.13 ± 0.37	2.63 ± 0.45	1.02 ± 0.24	1.25 ± 0.15	1.17 ± 0.31	1.23 ± 0.25
	18:1-20:4 (Diacyl)	2.43 ± 0.24	2.27 ± 0.33	1.30 ± 0.35	1.11 ± 0.23	0.95 ± 0.30	1.11 ± 0.33
	18:0-20:4 (Diacyl)	2.41 ± 0.38	2.25 ± 0.35	1.11 ± 0.20	1.84 ± 0.22	1.49 ± 0.32	1.70 ± 0.30
PI_DHA_Acyl	18:0-22:6 (Diacyl)	1.64 ± 0.12	1.75 ± 0.29	0.73 ± 0.23	1.96 ± 0.16	1.43 ± 0.58	1.54 ± 0.17

*$p < 0.05$